

Age constraints and provenance of the Mount Bischoff inlier and the Luina Group: evidence from LA-ICPMS U-Pb dating of detrital zircon

by Grace Cumming, J. L. Everard and S. Meffre





Mineral Resources Tasmania

PO Box 56

Rosny Park Tasmania 7018

Phone (03) 6165 4800

Fax (03) 62338338

Email info@mrt.tas.gov.au

Internet www.mrt.tas.gov.au

September 2016

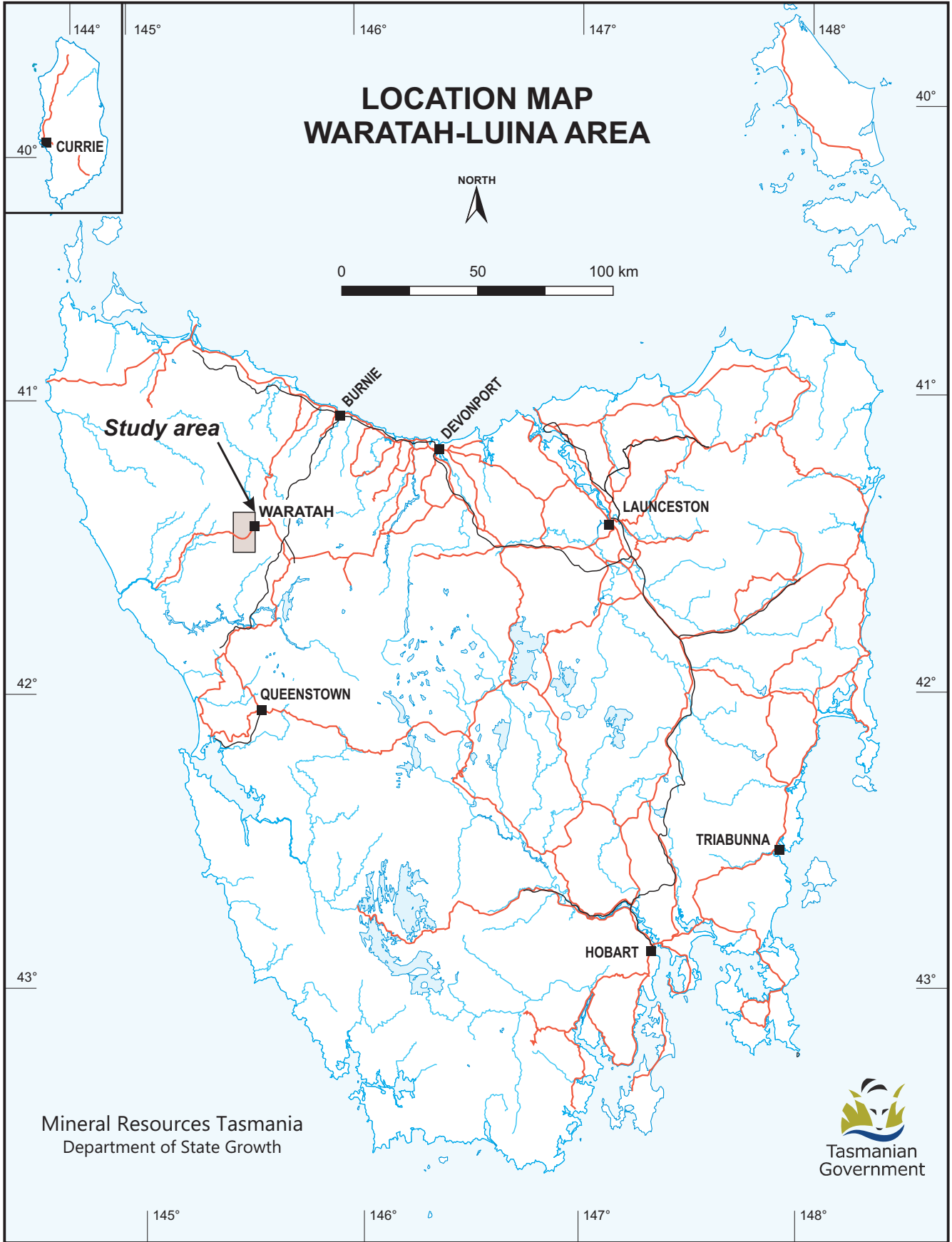
While every care has been taken in the preparation of this report, no warranty is given as to the correctness of the information and no liability is accepted for any statement or opinion or for any error or omission. No reader should act or fail to act on the basis of any material contained herein. Readers should consult professional advisers. As a result the Crown in Right of the State of Tasmania and its employees, contractors and agents expressly disclaim all and any liability (including all liability from or attributable to any negligent or wrongful act or omission) to any persons whatsoever in respect of anything done or omitted to be done by any such person in reliance whether in whole or in part upon any of the material in this report.

Tasmanian Geological Survey Record UR2016/04

Age constraints and provenance of the Mount Bischoff inlier and the Luina Group: evidence from LA-ICPMS U-Pb dating of detrital zircon

by G. V. Cumming, J. L. Everard and S. Meffre

LOCATION MAP WARATAH-LUINA AREA



Mineral Resources Tasmania
Department of State Growth



Contents

List of figures.....	6
List of tables	6
List of appendices	6
Abstract	7
Introduction	7
Geological setting	7
Mount Bischoff inlier	8
Luina Group	8
Previous age constraints	9
Oonah Formation	9
Luina Group	10
Sample selection	11
Oonah Formation	11
Luina Group	14
Geochronology	14
Methods	14
Results	15
Mount Bischoff inlier (Oonah Formation correlative).....	21
Luina Group	21
Discussion	22
Mount Bischoff inlier (Oonah Formation correlative).....	22
Luina Group	22
Conclusion	23
Acknowledgements	24
References	24
Appendix	27

List of figures

Figure 1.	NW Tasmania showing the extent of Neoproterozoic to Cambrian rock units with the study area shown	8
Figure 2.	Geology of the Luina and Waratah area, including the Heazlewood River Ultramafic Complex, and sample and drill-hole locations.....	10
Figure 3.	Photographs showing thinly bedded pelites and more resistant ortho-quartz sandstones which were sampled for geochronology	11
Figure 4a.	Photomicrographs of dated samples, showing fine and coarse grained dominantly quartz sandstone	12
Figure 4b.	Photomicrographs of dated samples of volcanoclastic sandstone	12
Figure 4c.	Photomicrograph of dated samples of massive sandstone	12
Figure 5.	Geological map showing the location of drill-hole LD86-1 south of Luina	13
Figure 6.	Schematic grainsize log for drillcore LD86-1 showing the key lithologies and sample locations with median U-Pb detrital zircon ages for each	14
Figure 7.	Tera-Wasserburg plots of U-Pb zircon analyses for the Oonah Formation	15
Figure 8.	Tera-Wasserburg plots of U-Pb zircon analyses for the Oonah Formation	16
Figure 9.	Tera-Wasserburg plots of U-Pb zircon analyses for the Eldon and Luina Group	18
Figure 10.	Probability plots of U-Pb ICPMS ages of detrital zircons from the Luina-Waratah region	20

List of tables

Table 1.	Locations and rock types dated from the Bischoff inlier and the Luina Group	13
Table 2.	Summary of ages for Oonah Formation and the Luina Group	19

Abstract

Recent geological mapping has shown that the Waratah area, northwest Tasmania, is structurally complex, with numerous probable thrust-emplaced sedimentary and igneous units of inferred Proterozoic or Early Cambrian age. In order to better constrain the age of two poorly dated units, detrital zircon was extracted from two samples from the Mt Bischoff inlier and five samples from the Luina Group, and dated by the U-Pb method using laser ablation inductively coupled mass spectrometry (LA-ICPMS).

Results from the quartz sandstone samples from Mount Bischoff inlier indicate that they were deposited after ~1030 Ma. The detrital zircon age spectra are comparable to those previously obtained from the Oonah Formation, and support a previously suggested correlation with this unit, although they are also broadly similar to many other western Tasmanian Proterozoic successions. However, this age constraint is significantly younger than the 1100–1280 Ma maximum ages obtained from the Oonah Formation and correlatives elsewhere. Our data also suggest a fluid-flow event indicated by lead loss and metamict zircon ages at ~757 Ma, which may be an expression of the Wickham Orogeny.

Our results from the Luina Group indicate that it was deposited after ~536 Ma, and support a pre-Tyennan age (>510 Ma) inferred from field relations, thus tightly constraining its age as Early Cambrian. Two samples from volcanoclastic intervals within the locally lowermost unit, the Deep Creek Volcanics, contain only young (<583 Ma) zircons, which probably record a nearby episode of late Ediacaran felsic-intermediate volcanism. The overlying Halls Formation (one sample) and Crescent Spur Sandstone (two samples) are dominated by much older zircons, consistent with a progressively increasing influx of terrigenous material, probably from a more distal source. The age spectra of two of these samples have prominent peaks at 1700–1800 Ma and are similar to those of many Proterozoic

terrane in western Tasmania. The other sample from the Crescent Spur Sandstone has a quite different age profile with a broad peak at 1050–1150 Ma, a feature only previously observed in the Wings Sandstone from southern Tasmania.

Introduction

In the Waratah-Luina area, northwest Tasmania, two major structurally complex rock units are apparently unfossiliferous and, despite recent detailed geological mapping, their age is poorly constrained by geological relationships. The rocks of the fault-bounded Mount Bischoff inlier consist of lithological correlatives of the Oonah Formation, which elsewhere has been shown to be older than ca. 750 Ma and probably younger than ca. 1100 Ma (Black et al. 2004). An Early Cambrian age has been proposed for the Luina Group (previously known as the Cleveland-Waratah association; Brown 1989), but it has only confidently been shown to be older than ca. 510 Ma, and a correlation with the Neoproterozoic Crimson Creek Formation has also been suggested (e.g. Brown 1986).

In order to obtain better constraints on the depositional age and provenance of each unit, detrital zircons were separated from representative samples of each and dated by the U-Pb method, using laser ablation inductively coupled plasma mass spectrometry (LA-ICPMS).

Geological Setting

The distribution in northwest Tasmania of the Oonah Formation and correlatives, and the Luina Group, is shown in Figure 1.

Both the Mount Bischoff inlier and the Luina Group are structurally juxtaposed or interleaved with several slices of arc-related boninites, low-titanium tholeiites

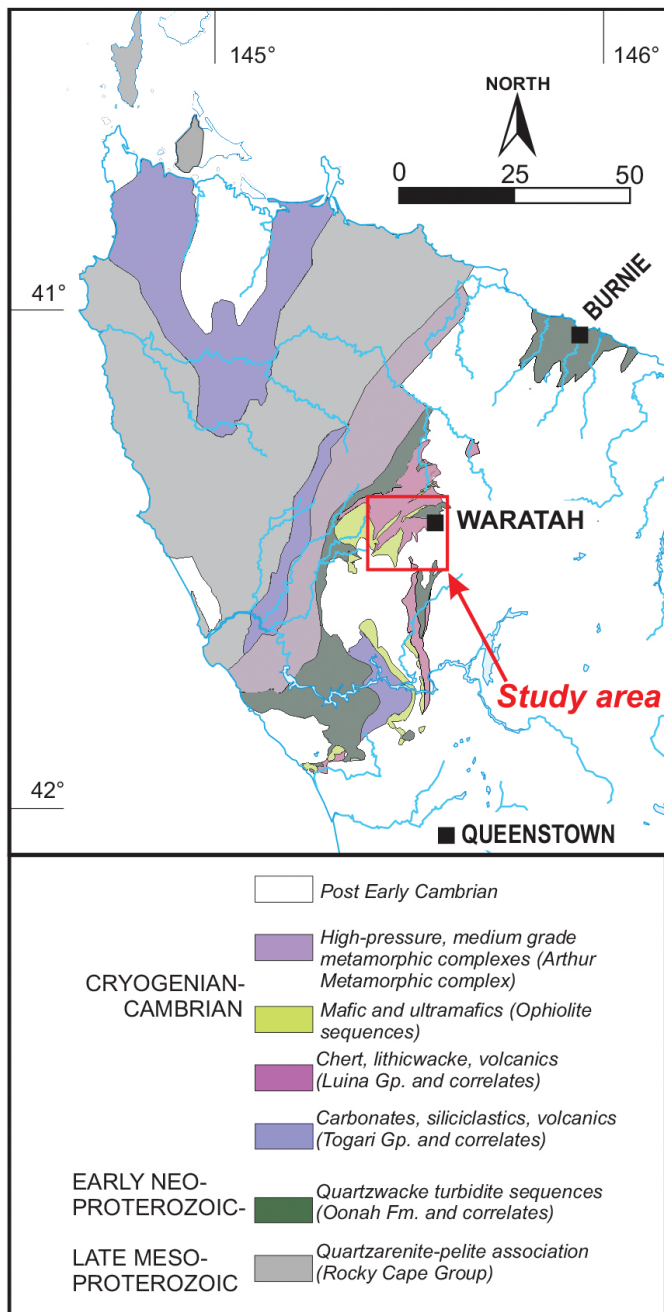


Figure 1. NW Tasmania showing the extent of Neoproterozoic to Cambrian rock units, with the study area shown.

and complementary ultramafics (including the Magnet, Whyte River and Heazlewood River complexes). These are considered to be the dismembered fragments of an ophiolite which was obducted westward over a passive margin, following an arc-continent collision at ca. 510 Ma, during an event known as the Tyennan Orogeny (Berry & Crawford 1988; Crawford & Berry 1992; Berry et al. 2007; Meffre et al. 2000; Chmielowski & Berry 2012; Mulder et al. 2016). The Waratah-Luina region is considered by Berry (2014) to lie in the “External Zone” or foreland of the obduction complex, in which

“relatively intact ophiolites sit on top of a relatively unmetamorphosed (very low grade) continental shelf sequence dominated by thin skinned deformation.”

The Luina Group is a probably allochthonous package of deep water sedimentary rocks, MORB-like rift tholeiite basalts and continentally-derived micaceous quartzwacke turbidites (e.g. Everard and Calver 2014). The Oonah Formation and correlatives consist mainly of continental turbidites with lesser pelite, dolostone and alkali basalt, and may represent parautochthonous thin-skinned slices of the passive margin, deformed and transported during the Tyennan Orogeny (e.g. Berry 2014).

Mount Bischoff inlier

The Mount Bischoff inlier crops out over about 17 km² immediately north of Waratah. It is bounded by faults just west of Arthur River, south of Deep Gully Creek and north of Ritchies Creek, and is overlapped by Tertiary basalt to the east. It comprises a 600-m-thick sequence of quartzite, siltstone and shale, overlain by a 60-m-thick unit of dolomite, followed by a 300-m-thick sequence of shale, siltstone and minor quartzite. The rocks of the Mt Bischoff inlier have undergone complex structural deformation and metamorphism (Groves 1969; Williams, in Seymour 1989). Folding of pelite and quartz sandstone beds is tight, especially directly adjacent to the margins of the inlier (Fig. 3). Williams (in Seymour 1989) identified two Proterozoic and two Devonian episodes of folding in the Mt Bischoff inlier. However, subsequent work elsewhere in Tasmania indicates that the earlier events (“Penguin Orogeny”) are probably Cambrian in age (Seymour & Calver 1995; Turner et al. 1998) and attributable to the Tyennan Orogeny.

The contact between the Mount Bischoff inlier and the enclosing Luina Group is complex. In drill-core (Fingerpost BH-1), the Oonah Formation near this contact comprises an interval of foliated black to grey, weakly carbonaceous mudstone, siltstone and quartzite. Elsewhere, the contact is marked by an extensive melange zone (up to 200 m across) in which a series of faults implies significant movement. Quartzite-pyrite clast breccias, of probable hydrothermal origin, crosscut the Oonah Formation above these fault zones.

Luina Group

The term Luina Group was formalised by Everard and Calver (2014) to apply to “the succession of sedimentary rocks and intercalated basalt north of the Heemskirk

Granite and east of the Heazlewood River Ultramafic Complex.” It comprises a thick sequence of lithicwacke sandstone, maroon volcanoclastic (locally shard-rich) siltstone, mudstone, chert and minor dolostone intercalated with tholeiitic, locally pillowed basalt flows. It is equivalent to the Luina Beds of Rubenach (1973) and Ford (1981), and the Arthur River sequence of Groves and Solomon (1964) and Groves (1968). These and subsequent workers (e.g. Brown 1986; Varne & Foden 1987) correlated these rocks with the Crimson Creek Formation, a lithologically similar sequence in the Pieman River-Renison Bell area (Blissett 1962). However, Brown and Jenner (1988) and Brown (1989), on the basis of basalt geochemistry (including unpublished Nd isotope data) and sedimentological differences, considered that they form a distinct succession with ocean-floor affinities, in contrast to the continentally derived Crimson Creek Formation. Brown (1989) applied the informal term “Cleveland-Waratah association” to these rocks.

Previous and recent mapping suggests the Luina Group extends northwards and generally dips and faces NW at Luina (Collins 1983; Everard 2003), and traces of fold axes generally strike NNE along the flanks of Magnet Range and towards Horizontal Creek, northwest of Waratah. To the northwest, the Luina Group is faulted against the Heazlewood River Ultramafic Complex and the Oonah Formation. The Luina Group extends northward to the Hellyer River near Parrawe and southward along the eastern margin of the Huskisson Syncline to the vicinity of Rosebery. Possible correlates occur near Ulverstone (the Barrington Chert and Motton Spilite), near Trial Harbour, in southwest Tasmania (the Mainwaring Group) and near Adamsfield (the Ragged Basin Complex).

In the vicinity of the Cleveland Mine at Luina, the designated type area of the Luina Group (Everard & Calver 2014), Collins (1983) recognised three formations. The Deep Creek Volcanics (tholeiitic basalt and intercalated mainly volcanoclastic sediment), is overlain by the Halls Formation (dominantly shale, greywacke, chert and dolomite), followed by the Crescent Spur Sandstone (micaceous quartz-rich lithicwacke and interbedded siltstone, mudstone and chert).

Subsequent geological mapping on the Luina and Waratah 1:25,000 sheets (Everard & Cumming 2016) has shown that these lithological groupings can be recognised away from the type area, but are not necessarily in the same stratigraphic order.

Previous age constraints

Oonah Formation

The type area of the Oonah Formation is northwest of Zeehan (Oonah Quartzite and Slate; Spry 1958; Blissett 1962). Probable correlatives are present on the northwest coast (Burnie Formation (e.g. Spry 1957; Gee 1968, 1977) and the north coast (Badger Head Group; Gee & Legge 1979). There are also several smaller, mainly fault-bounded inliers in western Tasmania, at Dundas (Concert Schist of Blissett 1962), Ramsay River (Brown 1986) and south of Macquarie Harbour (McClenaghan & Findlay 1989, 1993), as well as Mount Bischoff. Everard and Calver (2014), to simplify nomenclature, applied the term Oonah Formation to all these occurrences.

The age of the Oonah Formation is poorly constrained from geological relationships. In the Pieman River, within the type area, Taylor (1954) and Brown (1986) inferred an unconformable relationship between the Oonah Formation and the Success Creek Group, because of the greater structural complexity of the former. However, the actual contact (now beneath Lake Pieman) is faulted. The age of the Success Creek Group is indirectly constrained by a correlation with the Togari Group of the Smithton area, the base of which is ca. 750 Ma, based on carbon and strontium isotope chemostratigraphy (Calver 1998).

At Burnie, the Burnie (i.e. Oonah) Formation is intruded by sills of the Cooee Dolerite. Peperitic textures at the contact suggest that the dolerite was intruded into wet, unconsolidated sediment (Gee 1977; Crook 1979). However, a K-Ar biotite date of 711 ± 16 Ma (recalculated for new decay constants) from the Cooee Dolerite was interpreted as a minimum age due to possible argon loss (McDougall & Leggo 1965). Therefore it provides only a minimum depositional age for the Oonah Formation. Efforts to obtain a more robust radiometric date from the Cooee Dolerite have so far been unsuccessful (e.g. Black et al. 1997; Turner et al. 1998).

The relationship of the dominantly turbiditic Oonah Formation to the shelf succession of the Rocky Cape Group (Mesoproterozoic: Halpin et al. 2014) in far northwest Tasmania has been controversial. The two units are separated by the Arthur Metamorphic Complex, which contains higher grade equivalents of both, but are nowhere in unfaulted contact. Gee (1967) considered that the Burnie (Oonah) Formation is younger than the Rocky Cape Group and was possibly derived from it. Gee (1968) suggested, on general

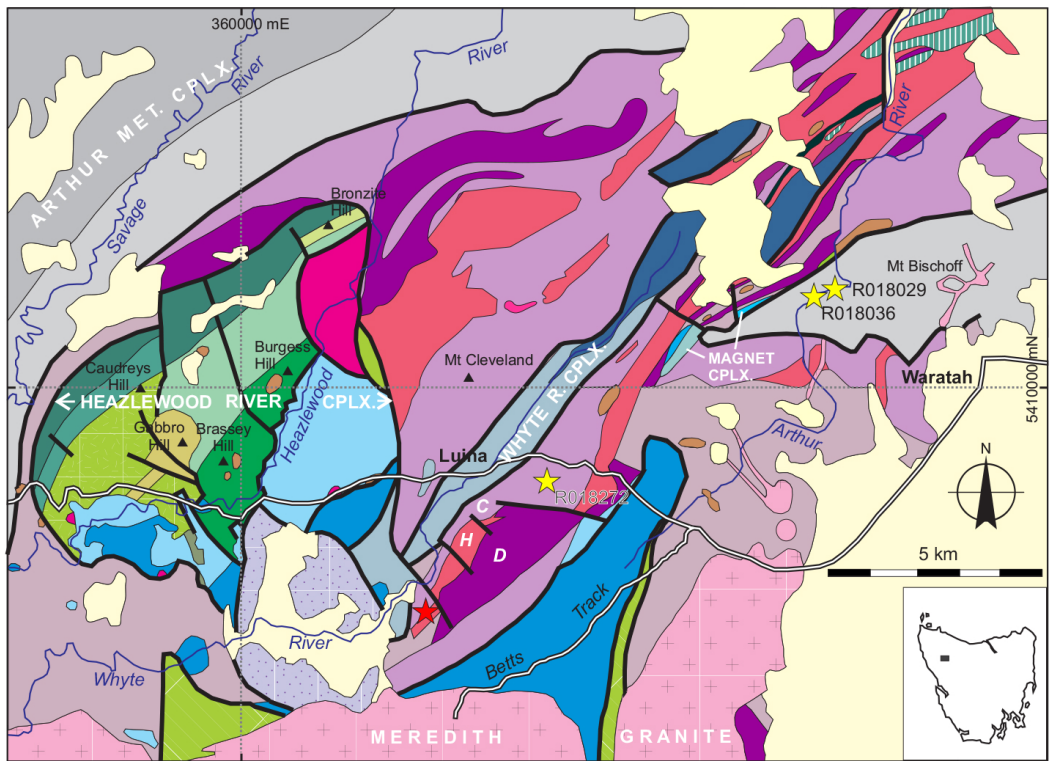
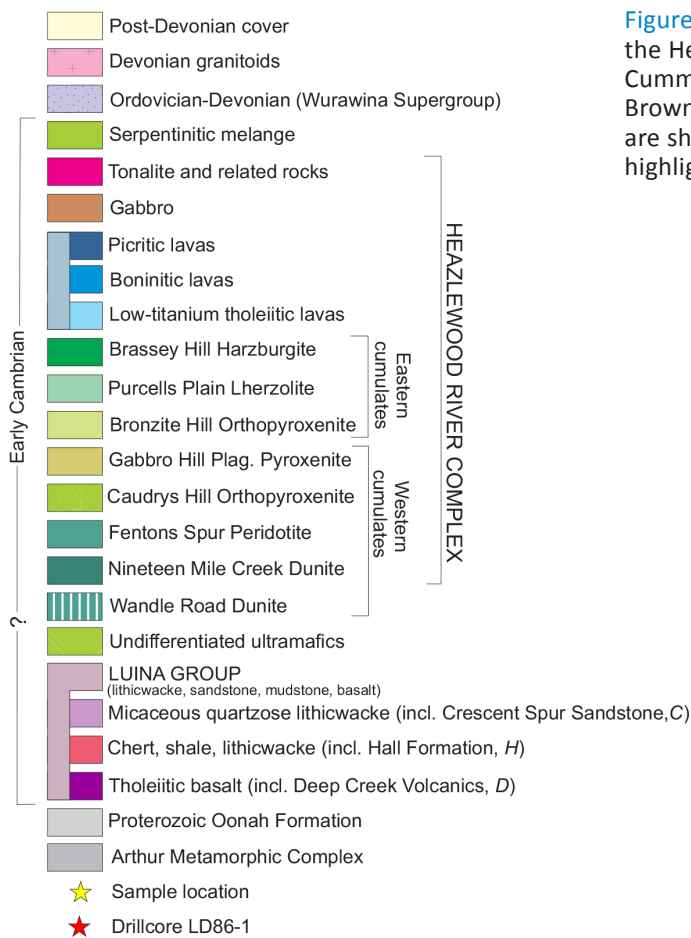


Figure 2. Geology of the Luina and Waratah area, including the Heazlewood River Ultramafic Complex. Adapted from Cumming and Everard (2016), Everard (2016), Collins (1983), Brown (1986) and Peck (1990). Sample and drill-hole location are shown as yellow and red stars and the key faults are highlighted as bold lines on the map.



structural grounds (e.g. eastward younging) that the Burnie (Oonah) Formation was probably younger than the Rocky Cape Group, “but onlaps it rather than overlies it.” In contrast, Turner et al. (1992, 1994) proposed a considerable time-span between the deposition of the Rocky Cape Group and that of the Burnie and Oonah Formations. He suggested that the Burnie (Oonah) Formation may be a much thicker distal turbiditic equivalent to basal shallow-water siliciclastic rocks (Forest Formation) in the Togari Group of the Smithton Synclinorium, and to the Donaldson Formation at the base of the Ahrberg Group. Both of these sequences are mid-Cryogenian in age and rest unconformably on the Rocky Cape Group (Seymour and Calver 1995).

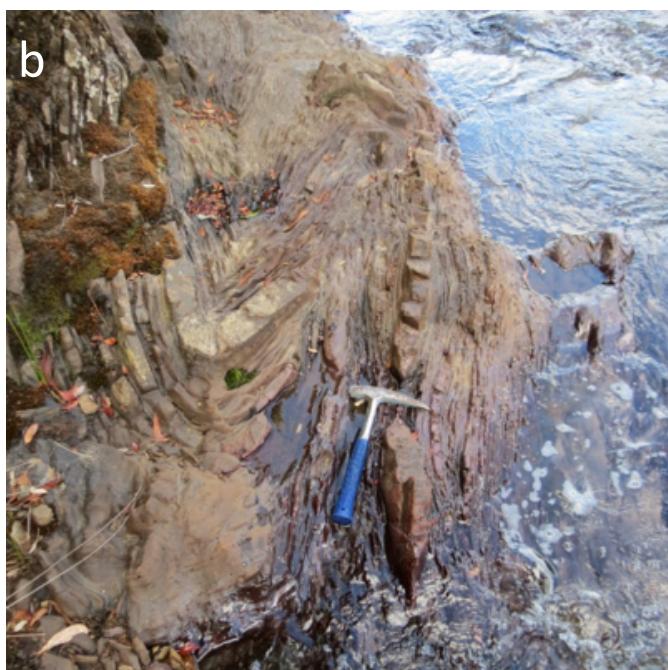


Figure 3. Photographs showing thinly bedded pelites and more resistant ortho-quartz sandstones which were sampled for geochronology. Samples were selected from Arthur River (sample R018036; shown in photograph a) and Magnet Creek (R018029; shown in photograph b).

A previous detrital zircon study, aimed at constraining the deposition age and provenance of predominantly western Tasmanian Proterozoic successions (Black et al. 2004), included three samples of the Oonah Formation and correlatives. A sample from Montana Flats, near the type area, yielded two zircons with an “imprecisely defined” age of ca. 1200 Ma. The two youngest zircons from a sample from the Heazlewood River (near Savage River township and about 20 km WSW of the Mt Bischoff

inlier) were ca. 1280 Ma. A sample from the Badger Head inlier on the north coast contained a single zircon of ca. 1100 Ma “which in isolation does not provide a precise temporal constraint for deposition” which was “better achieved by the nine next oldest grains, which yield an age of 1242 ± 29 Ma.” All three samples yielded complex but similar age spectra of older zircons, with prominent components at ca. 1435–1470 Ma and 1780–1790 Ma, and many Archean zircons.

Luina Group

A minimum age for the Luina Group can be inferred from the age of the allochthonous arc-related volcanic and ultramafic complexes, tectonically emplaced within it. In particular, igneous zircons from a tonalite, considered to represent the last stage of magmatism in the Heazlewood River Ultramafic Complex, gave a SHRIMP U-Pb age of 513.6 ± 5.0 Ma, using the QCNG standard (Black et al. 1997). These authors prefer this age to a previously obtained 510 ± 6 Ma age from the same sample, based on the SL13 standard (Turner et al. 1998).

Sample selection

Representative samples from the Mount Bischoff inlier and the Luina Group were collected during geological mapping of the region in the period 2012–2015 (Fig. 1) and logging of drill core. Seven samples of relatively coarse-grained clastic facies were selected for age dating purposes (Fig. 2). Sample details are given in Table 1.

Oonah Formation

A distinctive succession of massive quartzite, passing upwards into quartz sandstone, pelite and abundant shale is exposed along the Arthur River and at Mt Bischoff (Figs 2, 3). Two samples were collected from the western part of the inlier, about 1.6 km apart, from outcrop along the upper Arthur River (R018029) and Magnet Creek (R018036).

These lithic and quartz-rich sandstones (including greywacke and quartzite), and siltstones contain 70–90% clastic quartz grains, minor muscovite (2–10%), titanite and monazite (5%) set in a quartz and sericite matrix (Fig. 4a). Clastic grains measure up to 0.2 mm in diameter, with an average grain size of approximately 0.05 mm.

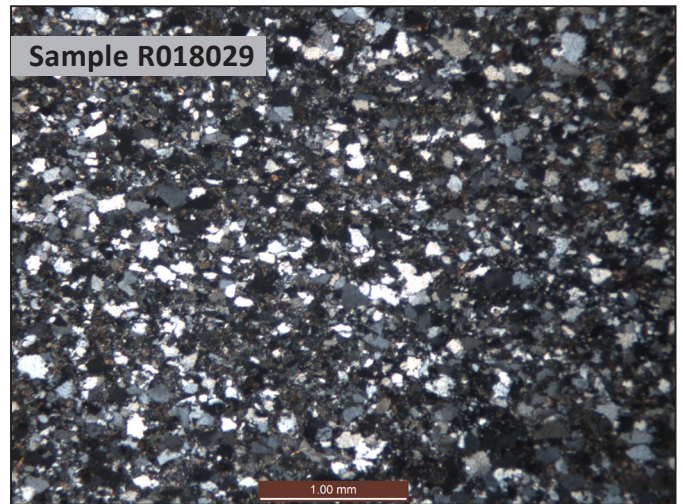
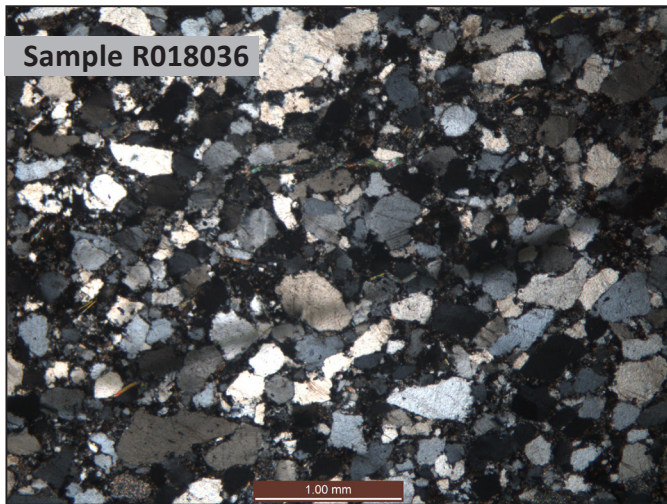


Figure 4a. Photomicrographs of dated samples, showing coarse (R018036) and fine (R018029) grained dominantly quartz sandstone (under cross polarised light).

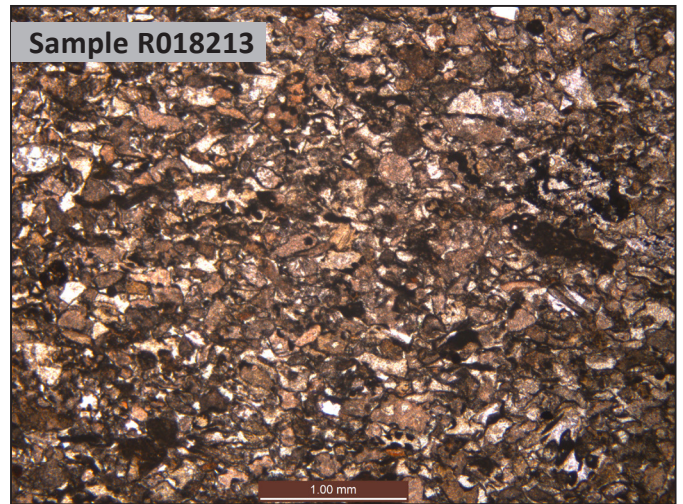
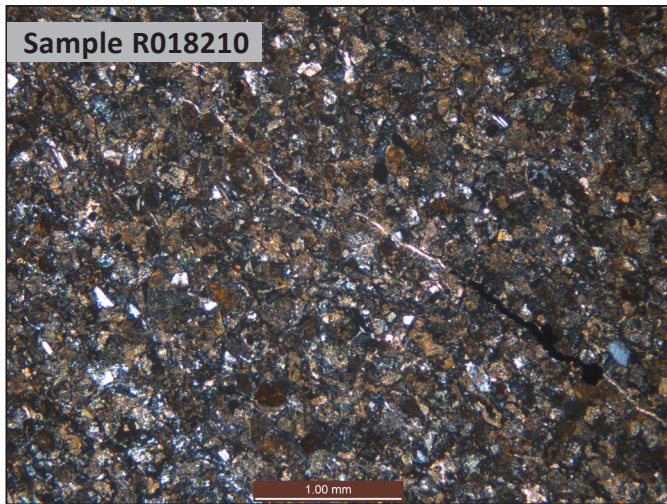


Figure 4b. Photomicrographs of dated samples of volcaniclastic sandstone (R018210 and R018213).

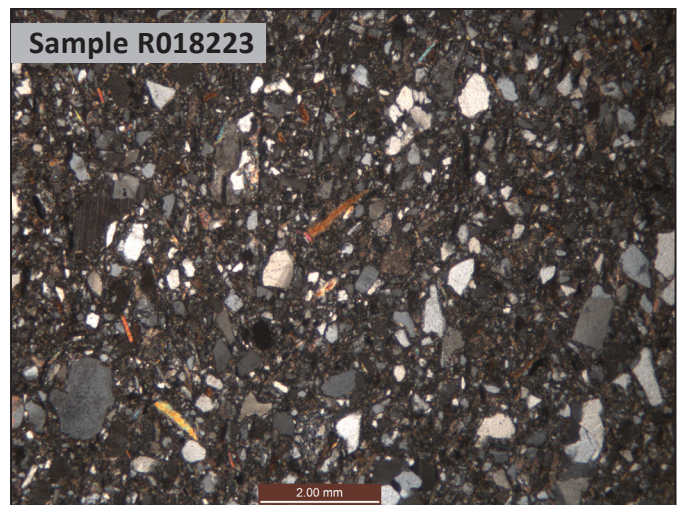
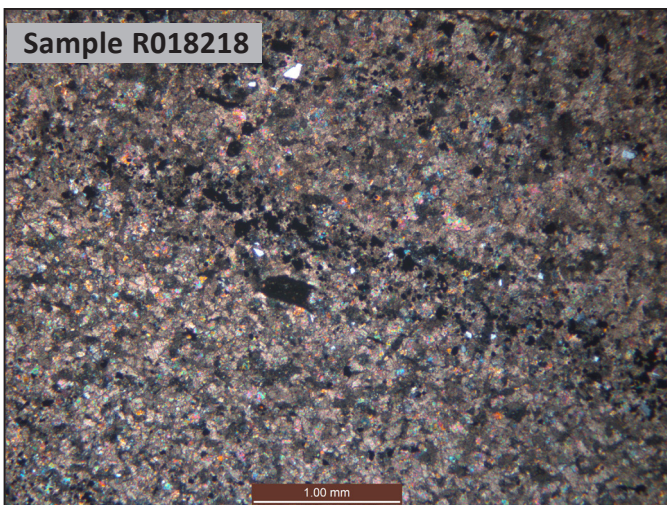


Figure 4c. Photomicrographs of dated samples of massive sandstone (R018218 and R018223).

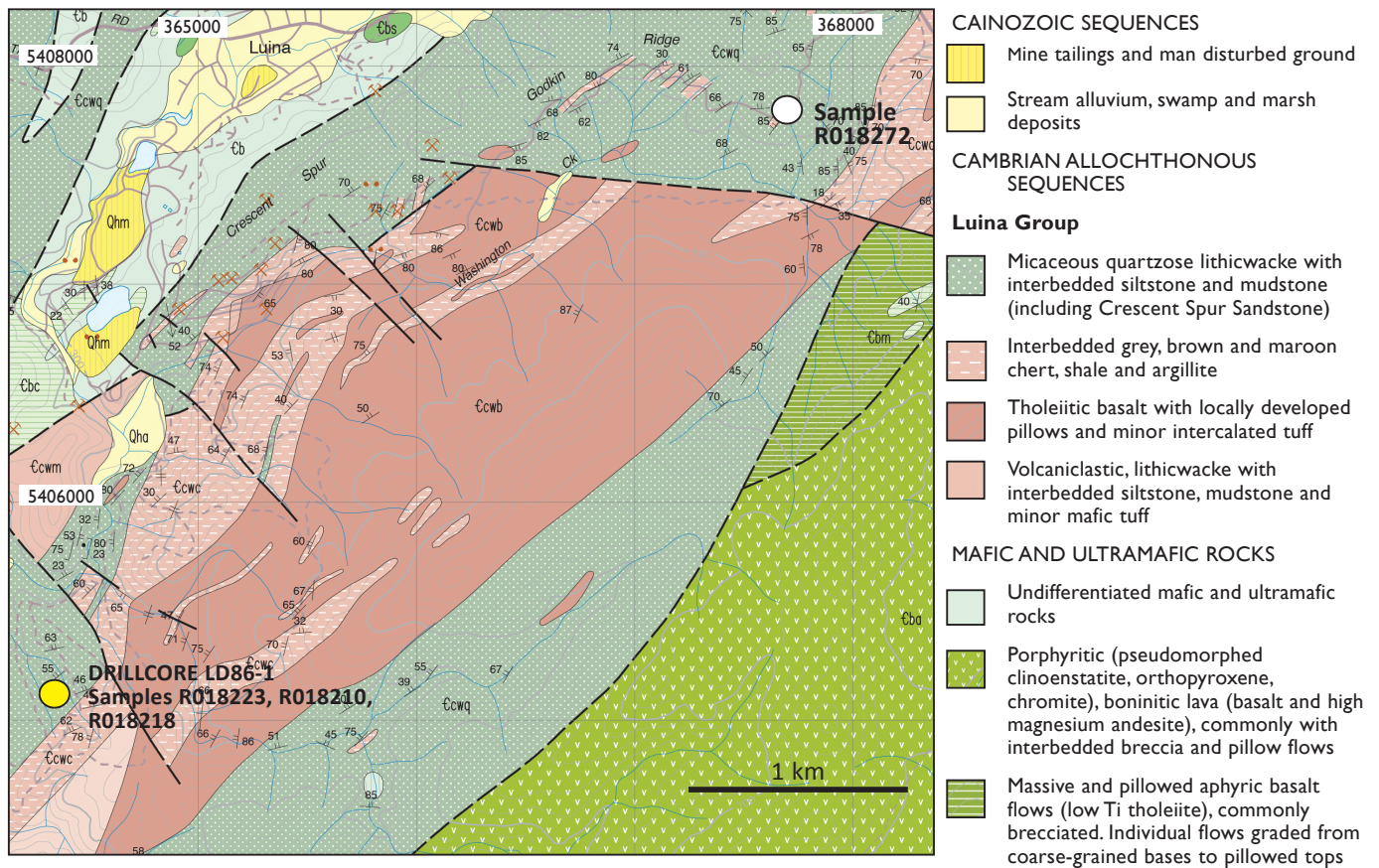


Figure 5. Geological map showing the location of drill-hole LD86-1 south of Luina. Samples R018223, R018210 and R018218 were selected from this core. Sample R018272 was collected from Godkin Ridge and its location is indicated on the map.

Table 1. Locations and rock types dated from the Bischoff inlier and the Luina Group

Sample Number	Locality (GDA94)	Rock Type	Stratigraphic Unit
R018036	372365mE/ 5411887mN	Massive sandstone	Oonah Formation
R018029	373837mE/ 5412538mN	Stratified quartzite	Oonah Formation
R018223	364312mE/ 5404984mN	Micaceous sandstone	Luina Group; Crescent Spur Sandstone (?)
R018218	364312mE/ 5404984mN	Massive sandstone	Luina Group; Halls Formation
R018210	364312mE/ 5404984mN	Massive volcaniclastic sandstone	Luina Group; Deep Creek Volcanics
R018213	364312mE/ 5404984mN	Volcaniclastic sandstone	Luina Group; Deep Creek Volcanics
R018272	367796mE/ 5408040mN	Micaceous lithicwacke	Luina Group; Crescent Spur Formation

Diamond drill hole **LD86-1**
 Located at 364312 mE/5404984 mN

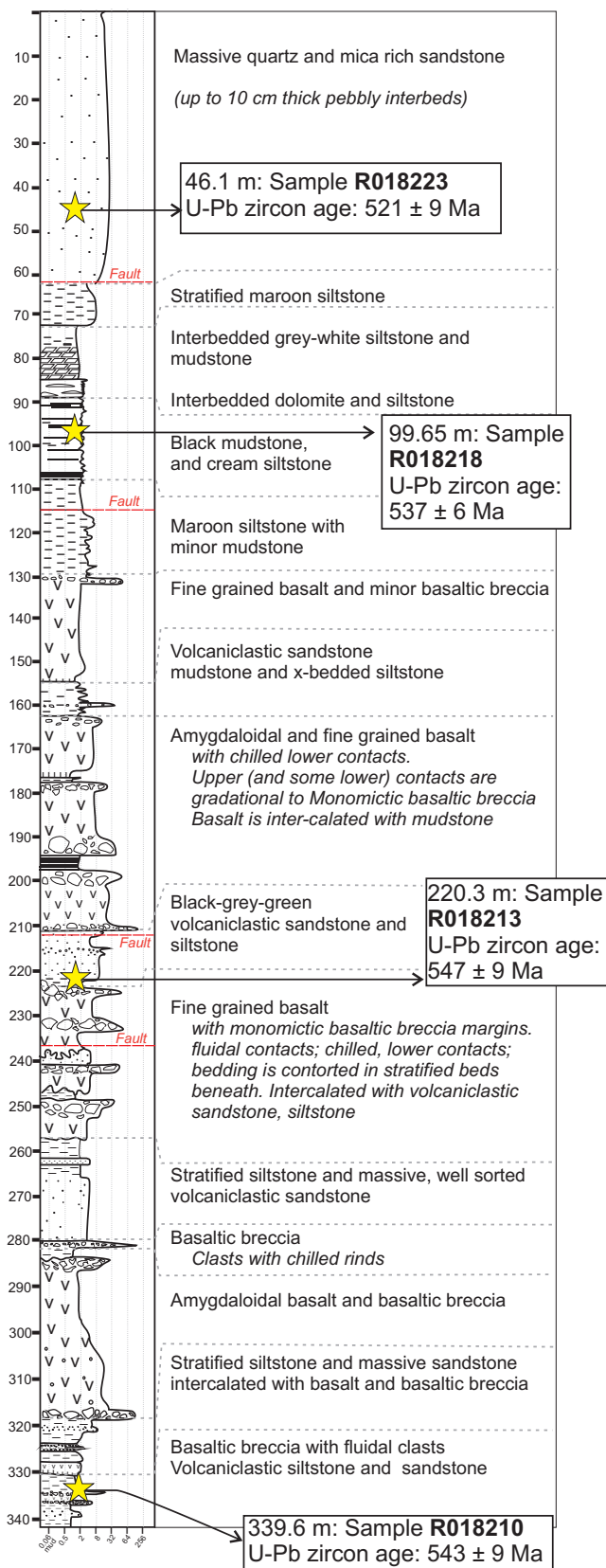


Figure 6. Schematic grainsize log for drillcore LD86-1 showing the key lithologies and sample locations with minimum U-Pb detrital zircon ages for each.

Luina Group

Four samples from the Luina Group were taken from core of hole LD86-1, drilled in 1986 by Billiton Australia about 3.3 km SSW of Luina. The hole was collared in the Crescent Spur Sandstone and plunged at 55° to 132°, approximately normal to local bedding which dips and faces to the northwest. However, stratigraphic relationships are somewhat uncertain due to at least four faults of unknown significance, identified in core (Figs 5, 6).

The hole initially passed through micaceous quartz sandstone, from which a sample (R018223) was taken at 46.1 m. At about 61 m, the hole encountered a faulted contact with a transitional interval of about 60 m of mixed volcanic and non-volcanic units, comprising interbedded maroon, grey-white, cream and black siltstone, mudstone and minor dolomite, referable to the Halls Formation. A sample (R018218) of a fine-grained non-volcanic, siltstone-dominant interval was taken at 99.65 m. From about 130 m to 342 m (end of hole) the core consists of dominantly basalt and basaltic breccia with intercalated volcaniclastic sandstone, siltstone and mudstone, referable to the Deep Creek Volcanics. Two samples (R018213, R018210) of glass shard and lithic-rich volcaniclastic sandstone (Fig. 4b) were selected (220.3–220.4 m and 336.2–337 m, respectively).

A second sample of micaceous lithicwacke (R018272) was taken from surface outcrop at Godkin Ridge near Crescent Spur (Fig. 4c). Exposures in this area, along Corinna Road on the northern flank of Godkin Ridge form the type section for the Crescent Spur Formation, where it is over 350 m thick (Collins 1983).

Geochronology

Methods

U-Pb geochronology was undertaken at the University of Tasmania using the LA-ICPMS technique. The zircons were separated using a gold pan and a hand magnet from 200 g of rock powder crushed to a coarse sand using a ring mill. The zircons were hand-picked from the non-magnetic concentrate, mounted in epoxy resin, polished using a clean lap, washed and analysed using an excimer (193 nm) laser fitted with a Resonetics M50 ablation cell and an Agilent 7500 quadrupole ICPMS. Samples were analysed using a 32 µm spot at 5 Hz and 2J cm². The 91500 Zircon (Wiedenbeck et al. 1995, 2005)

was used as a primary standard and the Temora, Gj1 and Plesovice zircons (Black et al. 2003; Jackson et al. 2004; Sláma et al. 2008) were used as a secondary standard. Pb-Pb mass bias was corrected using the NIST610 standard glass. Age calculations were performed using the techniques described in various University of Tasmania publications (e.g. Sack et al. 2011; Halpin et al. 2014).

Results

Numerical results for each sample are presented in Table 2 and graphically as plots of $^{238}\text{U}/^{206}\text{Pb}$ against $^{207}\text{Pb}/^{206}\text{Pb}$ (Figs 7, 8, 9) and $^{207}\text{Pb}/^{235}\text{U}$ against $^{206}\text{Pb}/^{238}\text{U}$ (Figs 7, 8), in each case with concordia curves shown.

For each individual zircon analysis, a “preferred age” was chosen based on the degree of discordance, the amount of common Pb and the age of the zircons. For many analyses, this is the $^{206}\text{Pb}/^{238}\text{U}$ age, where necessary corrected for common lead, using ^{207}Pb , to bring to concordia. In most cases, this correction is less than 10 m.y. For those analyses for which lead loss is identifiable, the preferred age has been taken as the $^{207}\text{Pb}/^{206}\text{Pb}$ age.

The preferred zircon ages from each sample are also presented in the form of an age spectrum (Fig. 10).

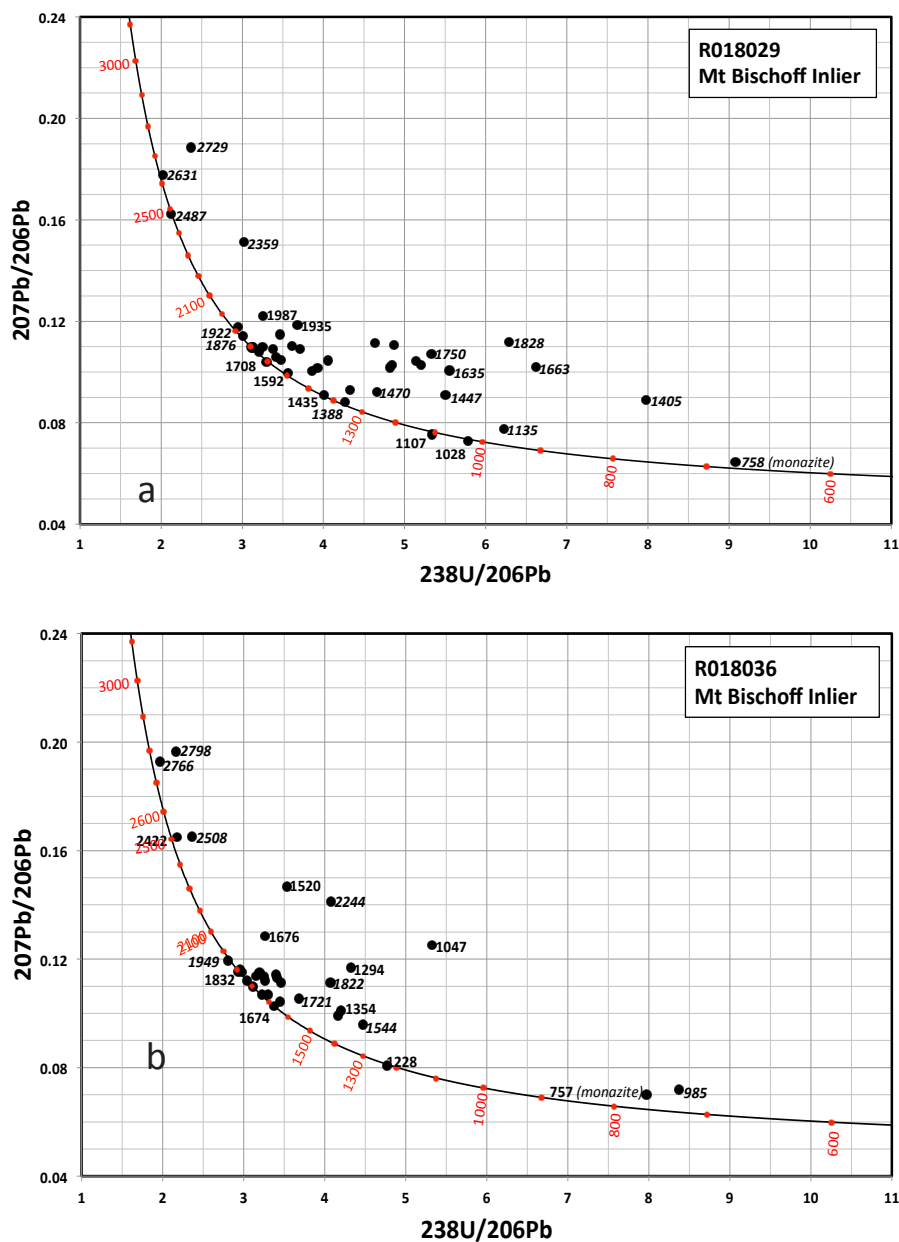
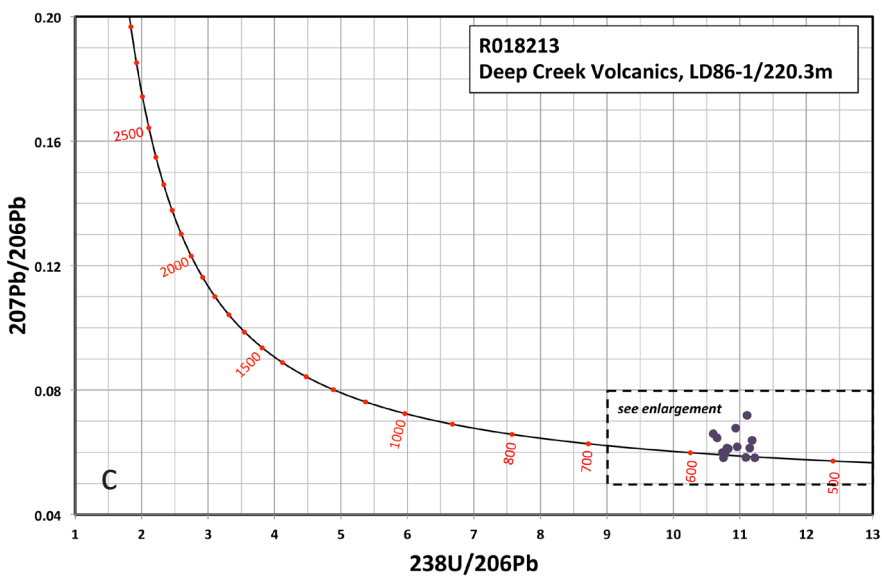
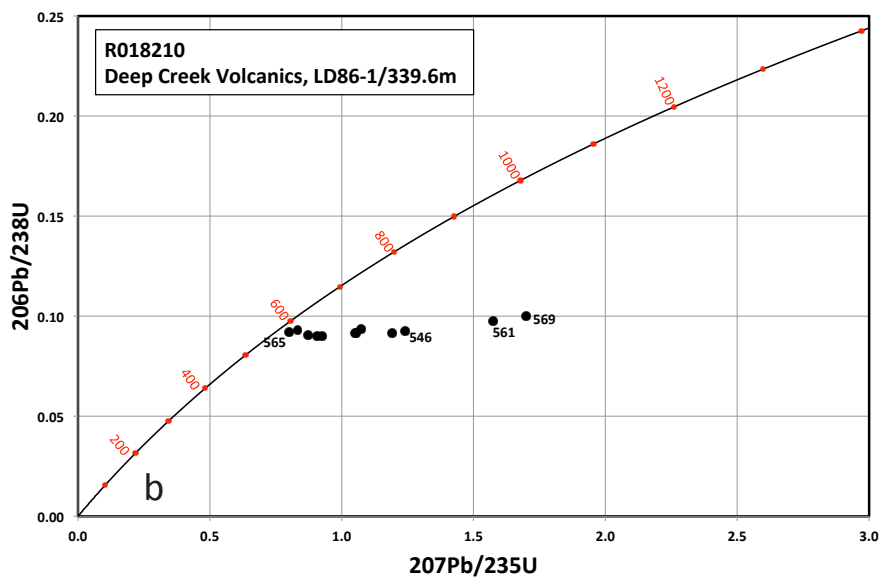
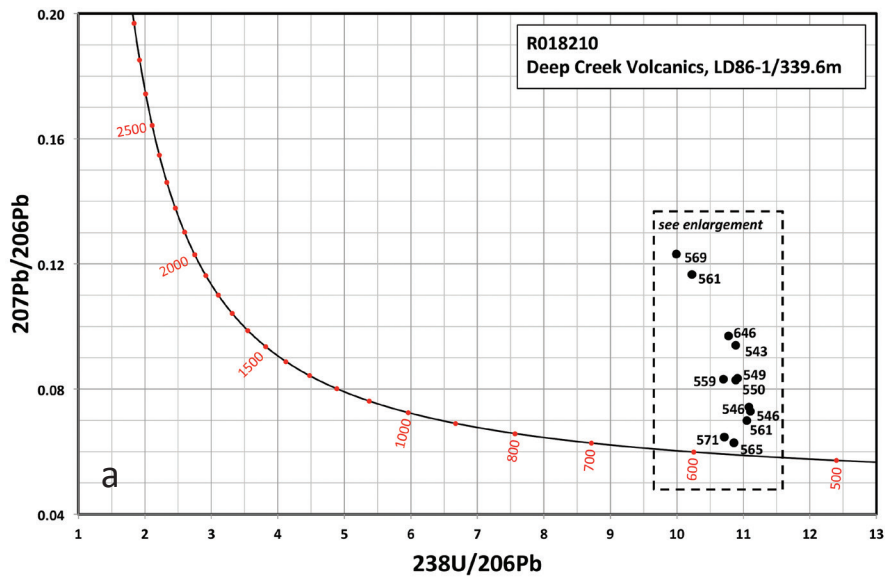


Figure 7. Tera-Wasserburg plots of U-Pb zircon analyses from the Oonah Formation. Individual $^{206}\text{Pb}/^{238}\text{U}$ ages are labelled in normal type and $^{207}\text{Pb}/^{206}\text{Pb}$ ages are in italics. A single monazite analysis from R018029 at 758 Ma and from R018036 at 757 Ma may relate to the Wickham Orogeny.



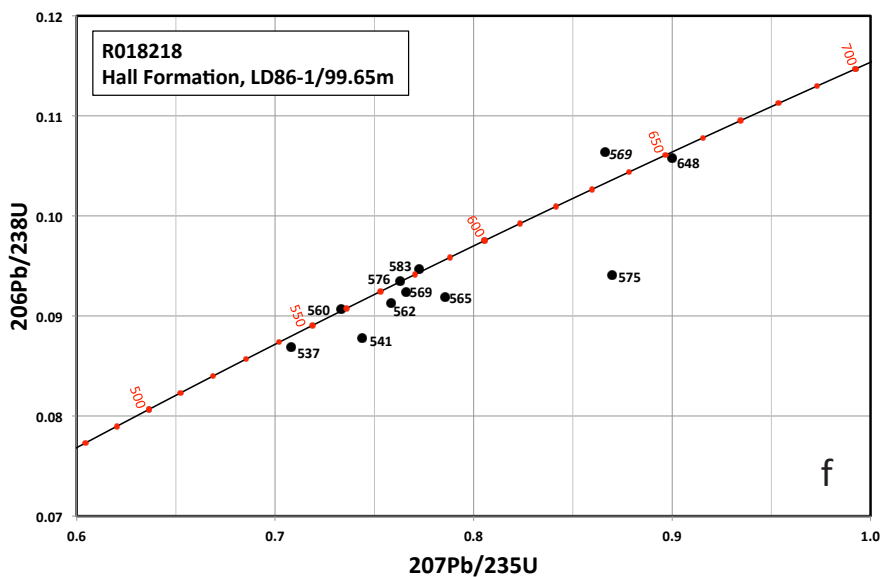
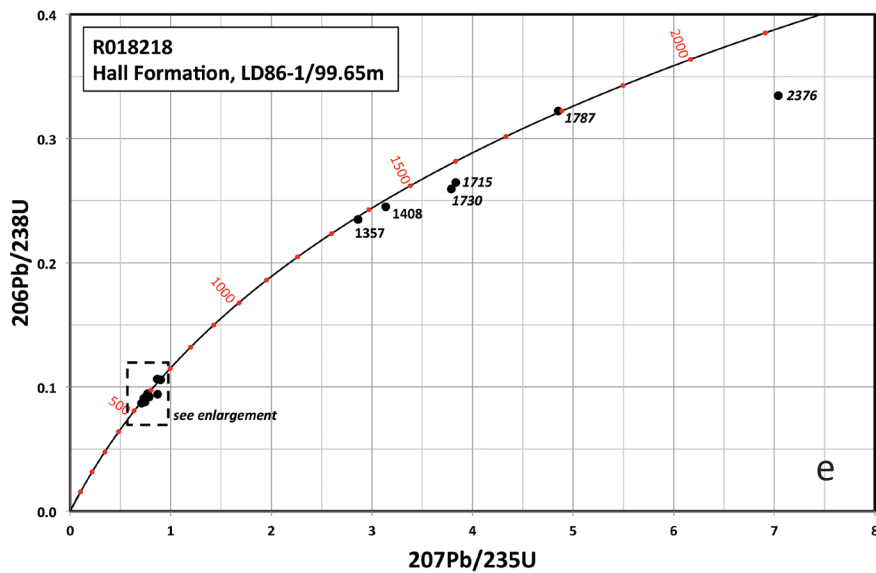
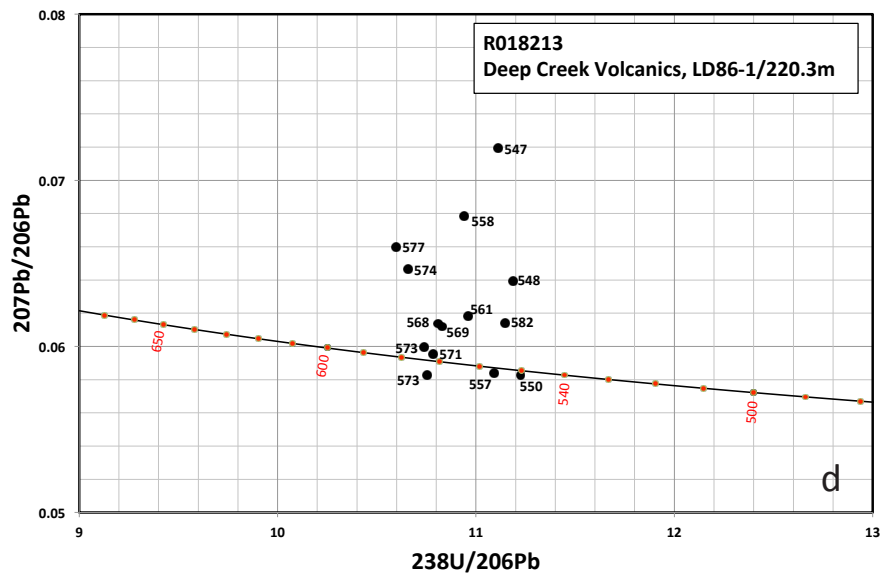
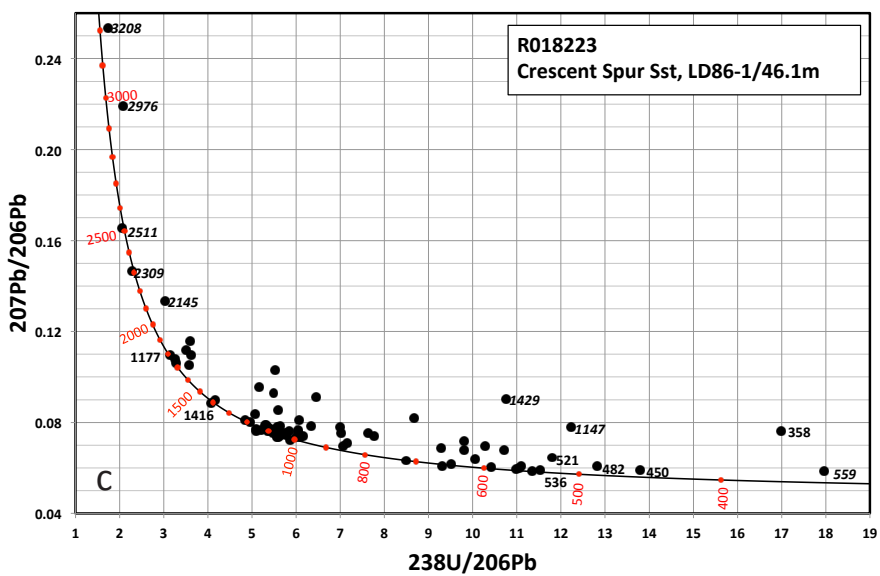
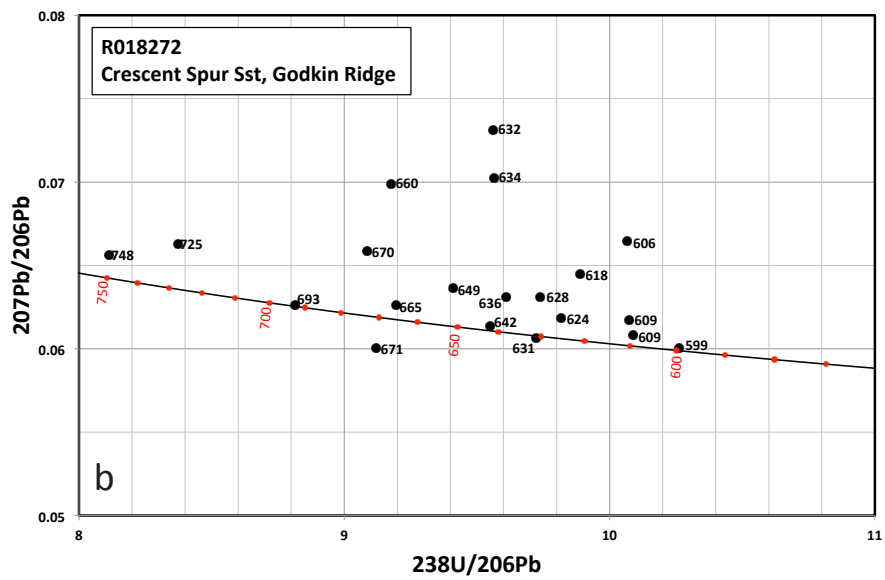
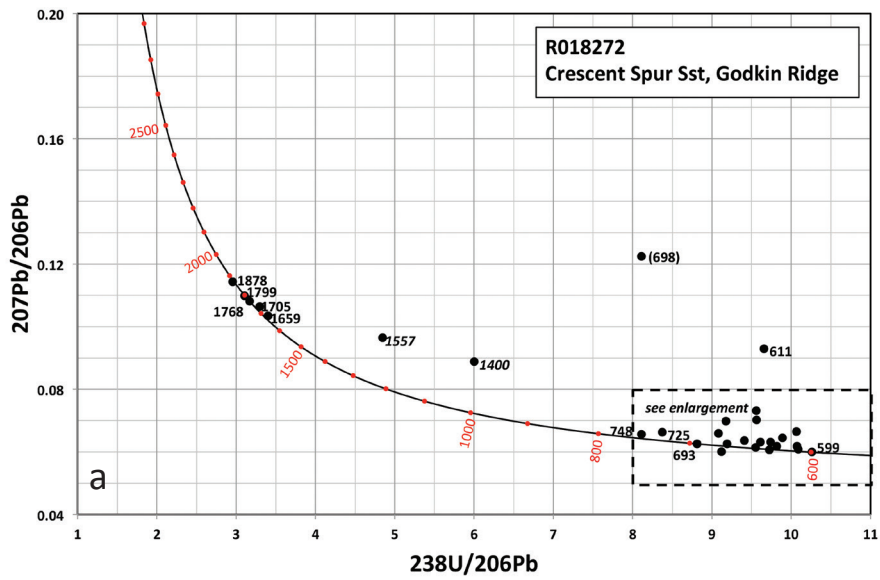


Figure 8 (a–f) Tera-Wasserburg plots of U-Pb zircon analyses for the Luina Group. Individual $^{206}\text{Pb}/^{238}\text{U}$ ages are labelled in normal type and $^{207}\text{Pb}/^{206}\text{Pb}$ ages are in italics. Analyses are scaled to show variability and zircons which are non-concordant for R018210, R018213 and R018218.



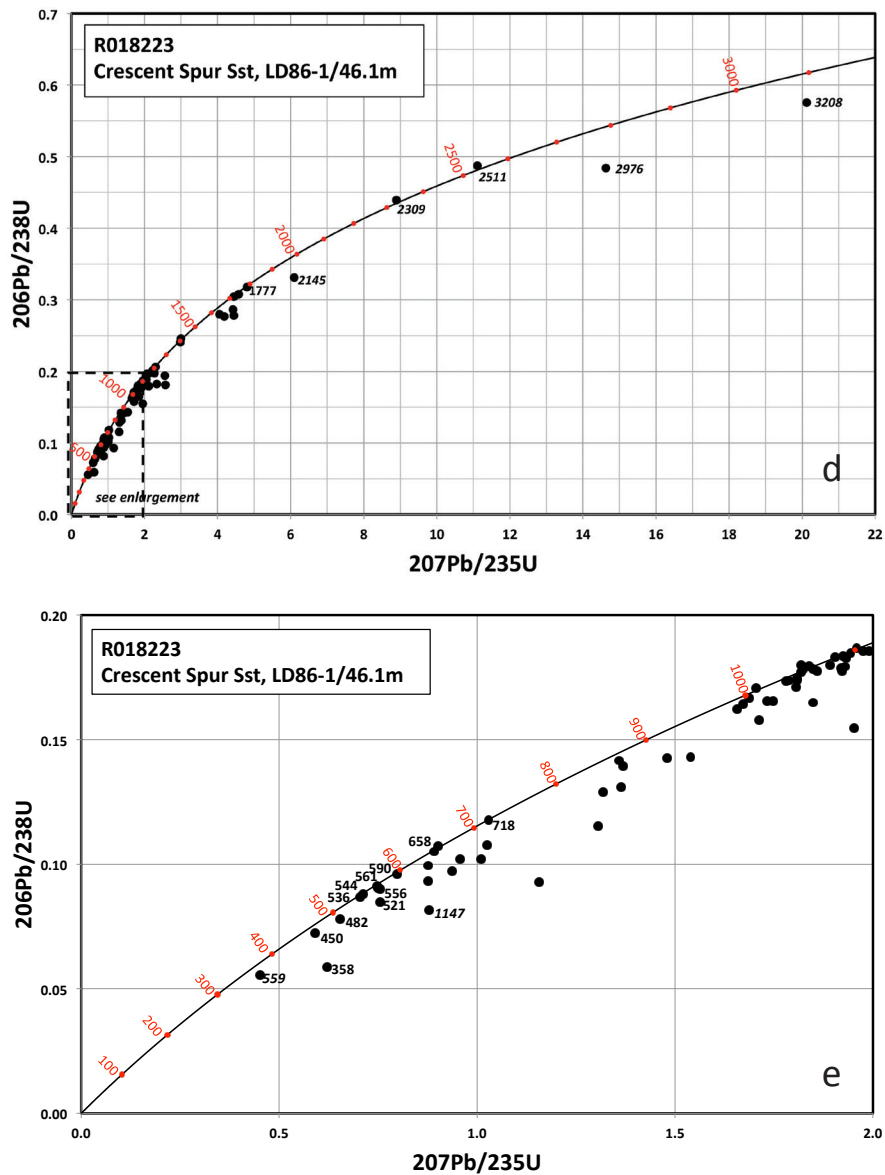


Figure 9 (a–e) Tera-Wasserburg plots of U-Pb zircon analyses for the Crescent Spur sandstone, which forms part of the Luina Group. Individual $^{206}\text{Pb}/^{238}\text{U}$ ages are labelled in normal type and $^{207}\text{Pb}/^{206}\text{Pb}$ ages are in italics. Analyses are re-scaled to show various non-concordant zircons in samples R018272 and R018223.

Table 2. Summary of ages for Oonah Formation and the Luina Group. All ages are U-Pb on zircon unless otherwise indicated.

Sample number	Rock type	Stratigraphic unit	Age	Median age (Ma)	Uncertainty (Ma)
R018036	Massive sandstone	Oonah Formation	757	1673.7	33
R018029	Stratified quartzite	Oonah Formation	758 on monazite	758	21
R018223	Micaceous sandstone	Luina Group; Crescent Spur Formation	358	450	11
R018218	Massive sandstone	Luina Group; Halls Formation	537	570.6	5.4
R018210	Massive volcanoclastic sandstone	Luina Group; Deep Creek Volcanics	543	556.3	6.7
R018213	Volcanoclastic sandstone	Luina Group; Deep Creek Volcanics	548	562.4	6.3
R018272	Micaceous lithicwacke	Luina Group; Crescent Spur Formation	599	613.5	7.3

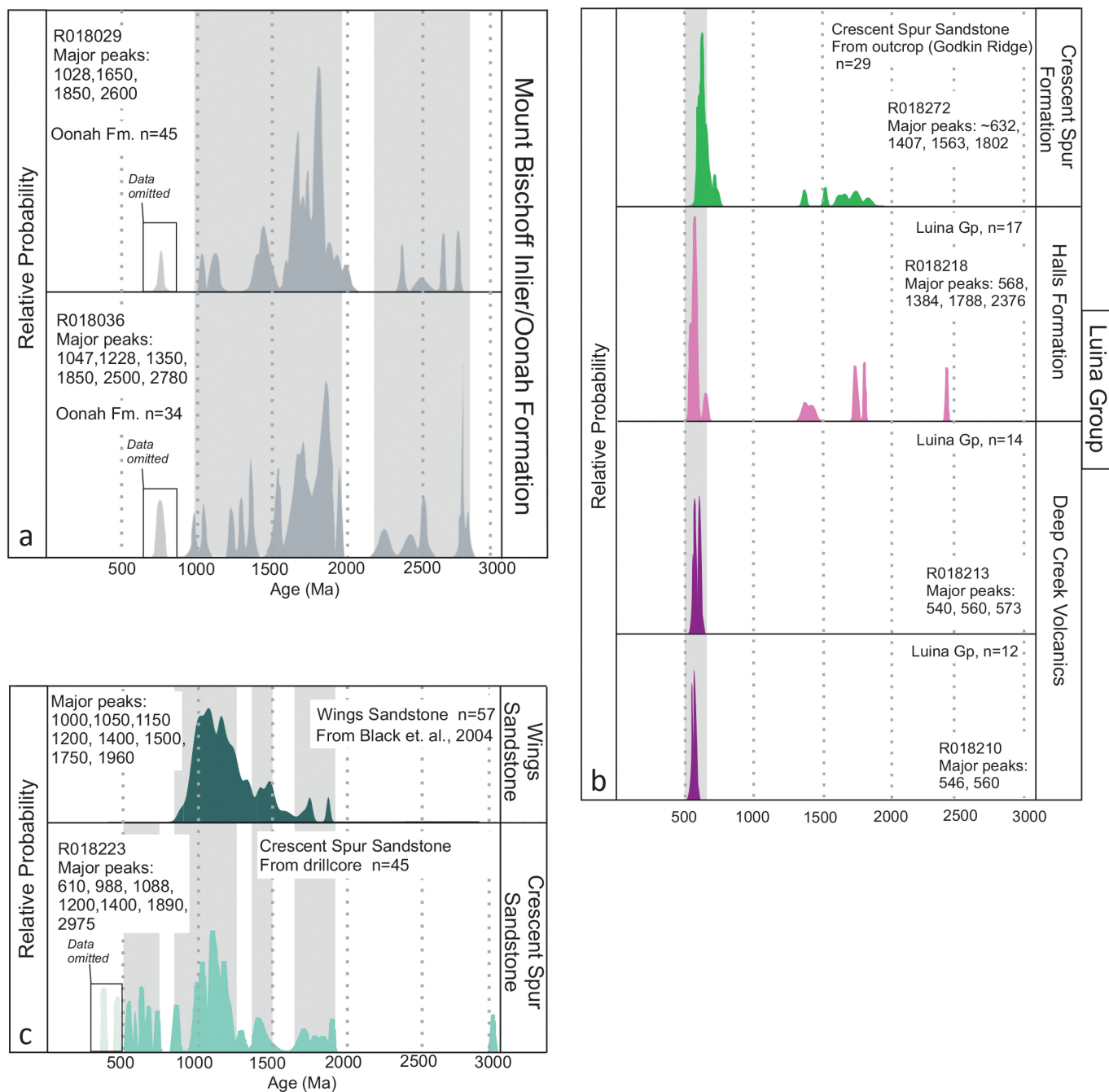


Figure 10. Probability plots of U-Pb ICPMS ages of detrital zircons from the Luina-Waratah region. (a) Probability plots for samples from the Oonah Formation. The 758 and 757 ages (as highlighted in the block on the left hand side) are omitted from the final age calculations. (b) The samples from the Luina Group show peak age ranges between 546 and 632 Ma and the volcanic dominated facies do not reveal any Paleo-Mesoproterozoic aged zircons. Samples from the Halls Formation and Crescent Spur Formation have similar detrital spectra. (c) The Wings Sandstone and sample R018223 from the Luina Group show a similar detrital spectrum between 1000 and 2000 Ma.

Mount Bischoff inlier (Oonah Formation correlative)

R018029

Many of the 45 grains analysed (including one monazite) exhibit lead loss, and for most the $^{207}\text{Pb}/^{206}\text{Pb}$ age is preferred.

The youngest grain is a single concordant monazite. Because of the absence of a monazite standard in the analytical run, the $^{207}\text{Pb}/^{206}\text{Pb}$ age of 758 ± 21 Ma is preferred as the $^{207}\text{Pb}/^{206}\text{Pb}$ system is not affected by mineral matrix effects. This is interpreted as an authigenic monazite that grew during the Wickham Orogeny (Berry 2014). Otherwise, the next youngest concordant grain is a zircon with a $^{206}\text{Pb}/^{238}\text{U}$ age (not requiring correction for common Pb) of 1028 ± 11 Ma. This provides a maximum depositional age for the sample. There is another similar concordant zircon at 1107 ± 13 Ma.

Most grains have ages between ca. 1400 Ma and ca. 2000 Ma. Many of these are discordant indicating Pb loss and thus the $^{207}\text{Pb}/^{206}\text{Pb}$ ages were mostly used. There are peaks in the age populations at ca. 1710 Ma and ca. 1800 Ma (with some concordant grains). There are four older grains with $^{207}\text{Pb}/^{206}\text{Pb}$ ages ranging from 2359 to 2729 Ma; the oldest concordant grain is 2487 ± 32 Ma ($^{206}\text{Pb}/^{238}\text{U}$).

R018036

Overall, the 34 grains show a similar age spectra to the other Oonah sample (R018029), although a somewhat higher proportion are concordant or nearly so. Generally $^{206}\text{Pb}/^{238}\text{U}$ ages are preferred for the relatively younger grains (ca. 1700 Ma) and $^{207}\text{Pb}/^{206}\text{Pb}$ ages for the older grains due to the presence of a small amount of Pb loss in the older grains.

The youngest apparent age is 757 ± 14 Ma from a metamict zircon exhibiting minor common lead. This age is interpreted to have been reset during the Wickham Orogeny, a feature also observed in some samples analysed by Black et al. (2004). There are also young zircons with ages of 985 ± 18 Ma (with lead loss and minor common lead, as well as very high Th and low Hf) and 1047 ± 15 Ma (markedly discordant with slight common lead). The youngest concordant zircon, however, yielded a $^{206}\text{Pb}/^{238}\text{U}$ age of 1228 ± 16 Ma.

There is a marked cluster of older ages, many concordant, between 1674 Ma and 1949 Ma with a peak at ca. 1850–1860 Ma. There are five older grains; the oldest with a $^{207}\text{Pb}/^{206}\text{Pb}$ age of 2798 Ma.

Luina Group

R018210 (Deep Creek Volcanics)

Twelve grains yield a narrow range of $^{206}\text{Pb}/^{238}\text{U}$ ages, from 543 to 571 Ma (late Ediacaran). However, most of the analyses are markedly discordant. On the $^{238}\text{U}/^{206}\text{Pb}$ against $^{207}\text{Pb}/^{206}\text{Pb}$ plot, an isochron anchored at the $^{207}\text{Pb}/^{206}\text{Pb}$ value for common lead in zircon yields an intercept age with the concordia curve of 556.3 ± 6.7 Ma (Fig. 10a).

R018213 (Deep Creek Volcanics)

Fourteen grains form a fairly close cluster at or close to concordia (Fig. 10b). The preferred $^{207}\text{Pb}/^{206}\text{Pb}$ ages, with slight (up to 9 m.y.) common lead corrections, yield an age range from 547 to 577 Ma. Although this sample (R018213) was taken from ~200 m higher in the same drill-hole and, if the intervening fault is unimportant, is thus probably younger than R018210, this range is slightly older.

Both R018210 and R018213 yield simple detrital zircon age spectra (Fig. 10). In particular, neither yielded any Mesoproterozoic or older zircons. This may be due to the small number of analyses, but from the formula $P = (1-f)^N$ it is a simple matter to calculate that another age component (say, >600 Ma) would probably ($N < 0.5$) have been detected from 12 analyses ($N = 12$) if it comprised more than 5.6% ($f = 0.056$) of the population. If the data from R018210 and R018213 are considered together as a single population ($N = 26$), an unobserved component would probably comprise no more than 2.6% of the population.

R018218 (Halls Formation)

Seventeen detrital zircons were analysed. Ten span an earliest Cambrian to Ediacaran age range (537 to 583 Ma) closely similar to those from the lower volcanoclastic sandstones. Eight of these are close to concordance, one (at 575 Ma) is slightly discordant, and another is strongly reverse discordant with a preferred $^{207}\text{Pb}/^{206}\text{Pb}$ age of 569 Ma. Another grain yielded a significantly older (Cryogenian) concordant age of 648 Ma.

Six grains yielded much older Mesoproterozoic to Palaeoproterozoic ages, ranging from near concordant $^{207}\text{Pb}/^{206}\text{Pb}$ ages of 1357 Ma and 1408 Ma to discordant $^{207}\text{Pb}/^{206}\text{Pb}$ ages of up to 2376 Ma.

R018223 (Crescent Spur Sandstone from LD86-1)

Eighty-nine zircon grains from this sample were analysed in two sessions, because of some ambiguity in the interpretation of the data from the youngest zircons obtained from the first session.

There is a wide range of apparent ages from 358 Ma (latest Devonian) to 3208 Ma (Archean), with a large cluster of concordant ages at ca. 950–1220 Ma. However, the three youngest ages have characteristics which suggest that the U-Pb isotopes in these analyses have been disturbed. The 358 Ma zircon has common lead, is slightly discordant and shows the highest U and Th values of any zircons analysed from the sample (R018223). The 450 Ma zircon also shows slight Pb loss and although concordant, its time-resolved depth profile varies between 350 and 470 Ma and was hence considered unreliable. The 482 Ma zircon is also affected by lead loss. Accordingly, these ages are rejected. The next youngest zircon, at 521 Ma, is slightly discordant due to the presence of common lead, but may provide an Early Cambrian maximum depositional age for this sample. The youngest completely concordant zircons yield $^{206}\text{Pb}/^{238}\text{U}$ ages of 536 and 544 Ma.

As well as the cluster of mostly concordant ages at ca. 980–1100 Ma, there is another possible smaller cluster at ca. 1700–1800 Ma and five concordant or slightly discordant $^{207}\text{Pb}/^{206}\text{Pb}$ ages of 2145, 2309, 2511, 2976 and 3208 Ma.

R018272 (Crescent Spur Sandstone from Godkin Ridge)

Twenty-seven zircons yielded ages ranging from 599 Ma to 1878 Ma. There is a large cluster of mostly concordant or near-concordant ages of 599 Ma to 693 Ma, and another two near-concordant zircons at 725 Ma and 747 Ma. Two strongly discordant zircons yielded $^{207}\text{Pb}/^{206}\text{Pb}$ ages of 1400 Ma and 1557 Ma, but the five oldest zircons are nearly concordant, with Palaeoproterozoic ages ranging from 1659 Ma to 1878 Ma (Fig. 10).

Discussion

Mt Bischoff inlier (Oonah Formation correlative)

The youngest reliable zircon ages from the two samples, particularly the concordant 1028 ± 11 Ma age from R018029, provide a latest Mesoproterozoic maximum depositional age for the Mount Bischoff inlier. This is significantly younger than the maximum ages of ~1100 Ma, ~1200 Ma and ~1280 Ma recorded from the Oonah Formation (and correlates) at Badger Head, Montana Flats and Heazlewood River respectively (Black et al. 2004).

The age spectra, with strong peaks between ~1710 and ~1860 Ma, tend to support the correlation with the Oonah Formation, although many western Tasmanian Proterozoic rocks have a similar zircon age profile (Black et al. 2004). The absence of any clear evidence for ~760 Ma igneous zircon tends to discount the alternative correlation with the Forest Conglomerate and the Donaldson Formation, since Cryogenian granites which might be expected to shed zircon of this age are known in the Bowry Formation (777 ± 7 Ma) and on King Island ($748 \pm$ and $760 \pm$ Ma) (Turner et al. 1998; Black et al. 1997). We have preferred to interpret monazite and metamict zircon grains of that age in this sample as crystallisation or resetting during the Wickham Orogeny. It is also noteworthy that the Forest Conglomerate itself failed to yield any zircons younger than ca. 1300 Ma, despite a ~750 Ma depositional age (Berry et al. 2001).

Zircons younger than 1047 Ma are generally absent in the Rocky Cape Group (Black et al. 2004; Halpin et al. 2014) although Black et al. (2004) noted a younger 1010 ± 45 population in the Jacob Quartzite. Sample (R018029) displays a small peak of ~1790 Ma zircon, similar to the Oonah Formation at Montana Flats and has similar 1600, 1700 and 1800 Ma peak ages to the Oonah Formation at Heazlewood (Black et al. 2004).

The samples also share peak 1450–1500 and 1850 Ma zircon ages with the Jacob Quartzite but lack the prominent 1245 Ma age. The age spectra show some similarity with that of the Detention Subgroup of the Rocky Cape Group as they both have peak ages centred around 1450 and 1750 Ma and contain Archean grains. The samples also share affinities with the lower-middle Rocky Cape Group as major age peaks between 1850 and 1830 are also present in the Balfour Subgroup (Halpin et al. 2014). The smaller age peak at 1650 Ma is present in most units within the Rocky Cape Group (except for the Detention Subgroup).

Luina Group

The youngest reliable zircon ages in each of the five samples are 543, 547, 537, 521 and 599 Ma. Given that the base of the Cambrian System has now been fairly accurately determined at 541.0 ± 1.0 Ma (Cohen et al. 2013), this data is consistent with an Early Cambrian age for the Luina Group. The possibility of a correlation with lithologically similar rocks in the Togari Group (Kanunnah Subgroup), and by extension the Crimson Creek Formation, is eliminated.

The absence of any zircon with Mt Read Volcanics ages (ca. 494–510 Ma; Black et al. 1997; Turner et al. 1998; Perkins & Walshe 1993; Mortensen et al. 2015) is consistent with a pre-Tyennan Orogeny (i.e. $>513.6 \pm 5$ Ma) age for the Luina Group.

The narrow age ranges of detrital zircons (543–571 Ma and 547–577 Ma) from the two volcaniclastic samples (R010210, R010213) from the Deep Creek Volcanics suggest that they were derived from a local, restricted, and probably intermediate to felsic volcanic source. However, the range in ages (28–29 m.y. for each sample) is probably too great to be attributable to analytical error (mostly 12–24 m.y. for each analysis; 2σ). This suggests that this phase of late Ediacaran volcanism probably lasted at least several million years, and was not a single short event.

Although the presence of intact and broken glass shards in these samples, together with the intercalated basalt and some relatively euhedral zircons, indicates syn-eruptive resedimentation, the older (up to 577 Ma) round to subhedral zircons suggest a detrital component from a slightly older volcanic terrain. These older zircons are approximately coeval with the onset of rift volcanism of the passive margin at 580–575 Ma, preserved in the Kanunnah Subgroup and on King Island (Everard & Calver 2014, p. 84). Although the bulk of this volcanism was basaltic, minor felsic activity, dated at 582 ± 4 Ma in northwest Tasmania and 575 ± 3 Ma on King Island (Calver et al. 2004), also occurred and may have provided a source of zircon.

The apparently overlying sample from the Halls Formation (R018218) also contains zircons with dominantly similar ages (537–583 Ma), but a scattering of older ages (1357–2376 Ma) appears to mark the influx of a component from an older, probably more distal and non-volcanic provenance. In the two samples (R018223 and R018272) of the Crescent Spur Sandstone, this older component is dominant.

Six of the thirteen older zircons in R018218 and R018272 have ages between 1700 and 1800 Ma. Zircons of this age are very common in western Tasmania Proterozoic successions, such as the Rocky Cape Group and Oonah Formation (Black et al. 2004; Halpin et al., 2014). These are potentially source areas for the Luina Group particularly the Crescent Spur Sandstone, which thus may have received terrigenous material from the passive margin shortly before the obduction event.

However, the other Crescent Spur Sandstone sample (R018223) has a very different zircon age profile, with a preponderance of Grenvillian zircon ages from 967 Ma to 1456 Ma and a broad peak between ca. 1050 and 1150 Ma. Zircons of this age are relatively rare in western Tasmania, but a similar age profile is displayed by the enigmatic Wings Sandstone, an east-dipping thrust slice outcropping near Adamsfield in southwest Tasmania. Before now, the detrital zircon distributions observed in the Wings Sandstone were unlike anything observed from any other unit in Tasmania (Black et al. 2004). However, the Wings Sandstone lacks any zircon younger than 914 ± 44 Ma (Black et al. 2004), whereas R018223 contains numerous zircons between 521 Ma and 898 Ma (Table 2). The data suggest that the Crescent Spur Sandstone south of Luina is probably derived (or derived in part) from a similar source area to the Wings Sandstone or a very similar correlate.

Another feature of this sample (R018223) is the three anomalously young apparent ages, particularly the 450 Ma and 482 Ma $^{207}\text{Pb}/^{206}\text{Pb}$ ages, which are only slightly discordant. An alternative explanation is that this sample, from the upper part of drill hole LD86-1, is a fault-bound outlier of the Eldon Group and may be related to the Crotty Formation. The Eldon Group contains Silurian fossils, and crops out about 1 km to the west. However, the Crotty correlative in that area (e.g. sample R017916) is a well-sorted quartz sandstone, very different from R018223. A second analytical session on this sample failed to reveal any similar young grains. The most likely explanation for these ages may be that they represent an old lead-loss event, possibly occurring during the Tyennan Orogeny at ca. 500–510 Ma.

Conclusion

Our new data demonstrate that the rocks of the Mount Bischoff inlier near Waratah are younger than ~ 1030 Ma. Although their detrital zircon age spectra support a correlation with the Oonah Formation (and are broadly similar to many other western Tasmania Proterozoic successions), this age constraint is significantly younger than the 1100–1280 Ma maximum ages obtained from the Oonah Formation and correlatives elsewhere. Zircons also reveal a fluid-flow event indicated by monazite, Pb loss and metamict zircon ages at ~ 757 Ma.

Our data also show that the Luina Group is Early Cambrian and no older than ~536 Ma, nor younger than ~510 Ma. Volcaniclastic intervals within the locally lowermost unit at Luina, the Deep Creek Volcanics, are dominated by young (<583 Ma) zircon probably recording a nearby episode of felsic-intermediate volcanism. The Halls Formation and the Crescent Spur Sandstone are dominated by much older zircon, recording an influx of terrigenous material, probably from a more distal source. The age spectra of two samples have prominent peaks at 1700–1800 Ma and are similar to that of many Proterozoic terranes in western Tasmania, but the third sample, from the Crescent Spur Sandstone, has an age profile only previously observed in the Wings Sandstone.

Additional synthesis of age data from the Oonah Formation by Black et al. (2004) and this study may help unravel the source region for the upper Mesoproterozoic stratigraphy in Tasmania.

At this stage further work is required to fully understand the timing and source characteristics of allochthonous units prior to their emplacement in the Early Cambrian. More detrital zircon age data may help to adequately define the nature and arrangement of sedimentary basins prior to the obduction and accretion of Tasmania to Gondwana in the Early Cambrian.

Acknowledgements

Jay Thompson and Jacqueline Halpin are acknowledged for undertaking the sample preparation, analysis and data reduction. Andrew McNeill is thanked for his encouragement to undertake the work and assistance with sample selection. Lia Unwin, Shane Heawood and Sam Poker are recognized for their assistance with the drill-core at the Mornington Core facility. Jacob Mulder is thanked for reading through the manuscript and providing invaluable comments and insight. Clive Calver is acknowledged and thanked for his invaluable insight and for his help to edit and improve the final draft. June Pongratz is gratefully acknowledged for her excellent editorial and compilation work.

References

- BERRY R. F. 2014. Cambrian Tectonics – The Tyennan Orogeny, *in*: CORBETT K. D.; QUILTY P. G.; CALVER C. R. (eds): *Geological Evolution of Tasmania. Geological Society of Australia Special Publication 24*: 34–94. Geological Society of Australia (Tasmania Division), Hobart, Tasmania. 639 pp.
- BERRY R.F.; CHMIELOWSKI R.M.; STEELE R.A.; MEFFRE R. 2007. Chemical U–Th–Pb monazite dating of the Cambrian Tyennan Orogeny, Tasmania. *Australian Journal of Earth Sciences* **54**: 757–771.
- BERRY R. F.; CRAWFORD A. J. 1988. The tectonic significance of Cambrian allochthonous maficultramafic complexes in Tasmania. *Australian Journal of Earth Sciences* **35**: 523–533.
- BERRY R. F., JENNER G. A., MEFFRE S. & TUBRETT M. N. 2001. A North American provenance for Neoproterozoic to Cambrian sandstones in Tasmania? *Earth and Planetary Science Letters* **192**: 207–222.
- BLACK L. P.; CALVER C. R.; SEYMOUR D. B.; REED A. 2004. SHRIMP UPb detrital zircon ages from Proterozoic and early Palaeozoic sandstones and their bearing on the early geological evolution of Tasmania. *Australian Journal of Earth Sciences* **51**: 885–900.
- BLACK L. P.; KAMO S. L.; ALLEN C. M.; ALEINIKOFF J. N.; DAVIS D. W.; KORSCH, R. J.; FOUDOULIS C. 2003. TEMORA 1: a new zircon standard for Phanerozoic U–Pb geochronology. *Chemical Geology* **200**: 155–170.
- BLACK L. P.; SEYMOUR D. B.; CORBETT K. D.; COX S. E.; STREIT J. E.; BOTTRILL R. S.; CALVER C. R.; EVERARD J. L.; GREEN G. R.; MCCLENAGHAN M. P.; PEMBERTON J.; TAHERI J.; TURNER N. J. 1997. Dating Tasmania's oldest geological events. *Australian Geological Survey Organisation Record* 1997/15.
- BLISSETT A. H. 1962. *1 Mile Geological Atlas Series Explanatory Report, Sheet 50 (7914S)*. Zeehan. Department of Mines, Tasmania.
- BROWN A. V. 1986. Geology of the Dundas–Mt Lindsay–Mt Youngbuck region. Tasmania Department of Mines Bulletin 62.
- BROWN A. V. 1989. Eocambrian–Middle Cambrian mafic volcanic rocks, *in* BURRETT C. F.; MARTIN E. L. (eds): *Geology and Mineral Resources of Tasmania. Geological Society of Australia Special Publication 15*: 61–69. Geological Society of Australia (Tasmania Division), Hobart, Tasmania. 639 pp.
- BROWN A. V.; JENNER G. A. 1988. Tectonic implications of the re-interpretation of Eocambrian Cambrian mafic volcanics and associated ultramafic rocks in western Tasmania, *in* TURNER N. J. (ed.): *The Geology and Evolution of the Latest Precambrian and Cambrian rocks in the Western Tasmania Terrane*. Abstracts Volume, 23–25. Geological Society of Australia (Tasmania Division).
- CALVER C. R. 1998. Isotope stratigraphy of the Neoproterozoic Togari Group, Tasmania. *Australian Journal of Earth Sciences* **45**: 865–874.
- CALVER C. R.; BLACK L. P.; EVERARD J. L.; SEYMOUR D. B. 2004. U–Pb zircon age constraints on late Neoproterozoic glaciation in Tasmania. *Geology* **32**: 893–896.
- CALVER C. R.; EVERARD J. L.; BERRY R. F.; BOTTRILL R. S.; SEYMOUR CHMIELOWSKI, R.M.; BERRY, R. F. 2012. The Cambrian metamorphic history of Tasmania: the metapelites. *Australian Journal of Earth Sciences* **59**: 1007–1019.
- COHEN K. M.; FINNEY S. C.; GIBBARD P. L.; FAN J.-X. 2013. The ICS International Chronostratigraphic Chart. *Episodes* **36**(3): 199–204.
- COLLINS P. L. F. 1983. *Geology and mineralisation at the Cleveland mine, western Tasmania*. PhD thesis, University of Tasmania.
- CRAWFORD A. J.; BERRY R. F. 1992. Tectonic implications of Late Proterozoic–Early Palaeozoic igneous rock associations in western Tasmania. *Tectonophysics* **214**: 37–56.
- CROOK K. A. W. 1979. Tectonic implications of some field relations of the Adelaidean Coee Dolerite, Tasmania. *Journal Geological Society of Australia* **26**: 353–361.

- CUMMING G. V.; EVERARD J. L. E. 2016. *Digital Geological Atlas 1:25 000 series, Sheet 3641. Waratah*. Mineral Resources Tasmania. In press.
- EVERARD J. L. (compiler) 2003. *Digital Geological Atlas 1:25 000 series, Sheet 3640, Luina*. Mineral Resources Tasmania.
- EVERARD J. L.; CALVER C. R. 2014. Early Cambrian allochthonous and paraautochthonous sequences, in CORBETT K. D.; QUILTY P. G.; CALVER C. R. (eds): *Geological Evolution of Tasmania. Geological Society of Australia Special Publication 24*: 110–141. Geological Society of Australia (Tasmania Division), Hobart, Tasmania. 639 pp.
- EVERARD J. L.; CUMMING G. V. 2016. *Digital Geological Atlas 1:25 000 series, Sheet 3640. Luina*. Mineral Resources Tasmania.
- FORD, R. J. 1981. Platinum-group minerals in Tasmania. *Economic Geology 76*: 498–504.
- GEE R. D. 1967. The Proterozoic rocks of the Rocky Cape Geanticline, in *The Geology of Western Tasmania — A Symposium*. University of Tasmania, Hobart.
- GEE R. D. 1968. A revised stratigraphy for the Precambrian in north-west Tasmania. *Papers & Proceedings of the Royal Society of Tasmania 102*: 7–10.
- GEE R. D. 1977. 1 Mile Geological Atlas 1 Series Explanatory Report, Sheet 22 (8015N). Burnie. Tasmania Department of Mines.
- GEE R. D.; LEGGE P. J. 1979. *Geological atlas 1:63,360 series, sheet 30 (8215N). Beaconsfield (2nd edn). Map and explanatory notes*. Tasmania Department of Mines.
- GROVES D. I. 1968. *The cassiterite-sulphide deposits of western Tasmania*. PhD thesis, University of Tasmania.
- GROVES D. I. 1969. The regional significance of the Don Hill fault zone of Mt. Bischoff, Tasmania. Geological Survey of Tasmania. Technical Report 14: 7–15
- GROVES D. I.; SOLOMON M. 1964. The geology of the Mt Bischoff district. *Papers and Proceedings of the Royal Society of Tasmania 98*: 1–22.
- HALPIN J. A.; JENSEN T.; MCGOLDRICK P.; MEFFRE S.; BERRY R. F.; EVERARD J. L.; CALVER, C. R.; THOMPSON J.; GOEMANN K.; WHITTAKER J. M., 2014. Authigenic monazite and detrital zircon dating from the Proterozoic Rocky Cape Group, Tasmania: Links to the Belt-Purcell Supergroup, North America. *Precambrian Research 250*: 50–67.
- JACKSON S. E.; PEARSON N. J.; GRIFFIN W. L.; BELOUSOVA E. A. 2004. The application of laser ablation-inductively coupled plasma-mass spectrometry to in situ U-Pb zircon geochronology. *Chemical Geology 211*: 47–69.
- McCLENAGHAN M. P.; FINDLAY R. H. 1989. *1: 50 000 Geological Atlas Series, Sheet 64 (7913S). Macquarie Harbour*. Department of Mines, Tasmania
- McCLENAGHAN M. P.; FINDLAY R. H. 1993. *1: 50 000 Geological Atlas Series Explanatory Report, Sheet 64 (7913S). Macquarie Harbour*. Department of Mines, Tasmania.
- MCDougall I.; LEGGO P. J. 1965. Isotopic age determinations on granitic rocks from Tasmania. *Journal of the Geological Society of Australia 12*: 295–332.
- MEFFRE S.; BERRY R. F.; HALL M. 2000. Cambrian metamorphic complexes in Tasmania: tectonic implications. *Australian Journal of Earth Sciences 47*: 971–985.
- MORTENSEN J. K.; GEMMELL J. B.; MCNEILL A. W.; FRIEDMAN R. M. 2015. High precision U-Pb chronostratigraphy of the Mount Read Volcanic belt in western Tasmania, Australia: implications for VHMS deposit formation. *Economic Geology 110*: 445–468.
- MULDER J. A.; BERRY R. F.; MEFFRE S.; HALPIN, J. A. 2016. The metamorphic sole of the western Tasmanian ophiolite: New insights into the Cambrian tectonic setting of the Gondwana Pacific margin. *Gondwana Research*, in press.
- PERKINS C.; WALSH J. L. 1993. Geochronology of the Mount Read Volcanics, Tasmania, Australia. *Economic Geology 88*: 1176–1197.
- RUBENACH M. J. 1973. *The Tasmania ultramafic-gabbro and ophiolite complexes*. PhD thesis, University of Tasmania.
- SACK P. J.; BERRY R. F.; MEFFRE S.; FALLOON T. J.; GEMMELL J. B.; FRIEDMAN R. M. 2011. In situ location and U-Pb dating of small zircon grains in igneous rocks using laser ablation-inductively coupled plasma-quadrupole mass spectrometry. *Geochemistry, Geophysics, Geosystems 12*(5), 23 pp.
- SEYMOUR D. B. 1989. *Geological Atlas 1:50 000 Series Explanatory Report. Sheet 36 (8015N). St Valentines*. Geological Survey Tasmania.
- SEYMOUR D. B.; CALVER C. R. 1995. Explanatory notes for the time-space diagram and stratotectonic elements map of Tasmania. Tasmanian Department of Development and Resources and the Australian Geological Survey Organisation and Tasmanian Geological Survey Record 1995/01, Hobart, Tasmania.
- SLÁMA J.; KOSLER J.; CONDON D. J.; CROWLEY J. L.; GERDES A.; HANCHAR J. M.; HORSTWOOD M. S. A.; MORRIS G. A.; NASDALA L.; NORBERG N.; SCHALTEGGER U.; SCHOENE B.; TUBRETT M. N.; WHITEHOUSE M. J. 2008. Plesovice zircon — A new natural reference material for U-Pb and Hf isotopic microanalysis. *Chemical Geology 249*: 1–35.
- SPRY A. H. 1957. The Precambrian rocks of Tasmania, Part I. Dolerites of the north-west coast of Tasmania. *Papers & Proceedings of the Royal Society of Tasmania 91*: 81–93.
- SPRY A. H. 1958. The Precambrian Rocks of Tasmania Part III: Mersey-Forth area. *Papers & Proceedings of the Royal Society of Tasmania 92*: 117–137.
- TAYLOR B. L. 1954. Progress report on the North Pieman mineral area. Unpublished report, Department of Mines Tasmania 1954: 149–203.
- TURNER N. J.; BLACK L. P.; KAMPERMAN M. 1994. Pre-Middle Cambrian stratigraphy, orogenesis and geochronology in western Tasmania, in COOKE D. R.; KITTO P. A. (eds): Contentious issues in Tasmanian geology. *Geological Society of Australia Abstracts 39*: 51–56.
- TURNER N. J.; BLACK L. P.; KAMPERMAN M. 1998. Dating of Neoproterozoic and Cambrian orogenies in Tasmania. *Australian Journal of Earth Sciences 45*: 789–806.
- TURNER N. J.; BOTTRILL R. S.; CRAWFORD A. J.; VILLA I. 1992. Geology and prospectivity of the Arthur Mobile Belt. *Geological Survey of Tasmania Bulletin 70*: 227–233.
- VARNE R.; FODEN J. 1987. Tectonic setting of cambrian rifting, volcanism and ophiolite formation in western Tasmania. *Tectonophysics 140*: 1–9.
- WIEDENBECK M.; ALLÉ P.; CORFU F.; GRIFFIN W. L.; MEIER M.; OBERLI F.; VON QUADT A.; RODDICK J. C.; SPEIGEL W. 1995. Three natural zircon standards for U-Th-Pb, Lu-Hf, trace-element and REE analyses. *Geostandards Newsletter 19*: 1–23.
- WIEDENBECK M.; HANCHAR J.; PECK W. H.; SYLVESTER P.; VALLEY J.; WHITEHOUSE M.; KRONZ A.; MORISHITA Y.; NASDALA L. 2005. Further characterization of the 91500 zircon crystal. *Geostandards and Geoanalytical Research 28*: 8–39.

blank

Table 2. Isotopic and age data from LA-ICPMS analysis of zircons in samples R018029 from the Mount Bischoff inlier.

Analysis	Preferred age	±1 ster	²⁰⁶ Pb/ ²³⁸ U age (²⁰⁷ corr)	±1 ster	²⁰⁶ Pb/ ²³⁸ U	±1 ster	²⁰⁷ Pb/ ²⁰⁶ Pb age	±1 ster	²⁰⁶ Pb/ ²³⁸ U ratio	±1 RSE	²⁰⁷ Pb/ ²⁰⁶ Pb ratio	±1 RSE	²⁰⁷ Pb/ ²³⁵ U ratio (calc)	²³⁸ U/ ²⁰⁶ Pb ratio	±1 std err	²⁰⁴ Pb (ppm)	²⁰⁶ Pb (ppm)	²⁰⁷ Pb (ppm)	²⁰⁸ Pb (ppm)	²³² Th (ppm)	²³⁸ U (ppm)	⁴⁹ Ti (ppm)	⁵⁶ Fe (ppm)	¹⁷⁸ Hf (ppm)	common Pb at age of zirc	²⁰⁸ Pb/ ²³² Th age	±1 ster	²⁰⁸ Pb/ ²³² Th ratio	±1 RSE	Notes		
R018029 (2013-391) Mt Bischoff inlier																																
AU21E132	758	11	671	6	673	6	758	11	0.110	0.9%	0.064	0.5%	0.979	9.08	0.09											0.883	646	8	0.032	1.2%	Monazite, use 7/6 age, Hg inclusion	
AU21E130	1028	11	1028	11	1028	11	1005	25	0.173	1.1%	0.073	1.2%	1.732	5.79	0.06	0.00	29	2	2	49	173	12	9	10432	0.911	1006	20	0.051	2.0%	ok		
AU21E133	1107	13	1107	13	1107	14	1078	36	0.187	1.2%	0.075	1.8%	1.948	5.34	0.07	0.01	12	1	2	34	63	30	2	10366	0.918	1050	21	0.053	2.0%	ok		
AU21E139	1135	14	954	9	961	9	1135	14	0.161	0.9%	0.078	0.7%	1.718	6.22	0.06	0.02	237	18	1	19	1587	13	1766	14080	0.905	1550	47	0.080	3.0%	Pb loss, slight 204		
SE18B270	1388	21	1357	20	1359	21	1388	21	0.235	1.5%	0.088	2.2%	2.855	4.26	0.06	0.00	14	1	5	83	63	7	39	8409	0.940	1319	21	0.067	1.6%	Pb loss in 2nd half		
AU21E138	1405	24	740	11	761	11	1405	24	0.125	1.5%	0.089	1.3%	1.539	7.98	0.12	0.00	96	9	5	121	740	27	1224	14199	0.889	772	23	0.039	3.0%	Pb loss, used lowest 204		
AU21E141	1435	14	1435	14	1435	15	1442	19	0.249	1.0%	0.091	1.0%	3.121	4.01	0.04	0.00	53	5	26	342	211	19	12	9813	0.947	1483	19	0.076	1.3%	ok		
AU21E115	1447	20	1057	13	1076	14	1447	20	0.182	1.3%	0.091	1.1%	2.280	5.50	0.07	0.02	39	4	10	139	209	27	65	9506	0.915	1429	22	0.073	1.5%	Pb loss, used lowest 204Pb		
AU21E119	1470	27	1239	17	1253	18	1470	27	0.215	1.4%	0.092	1.4%	2.726	4.66	0.07	0.03	57	5	8	137	298	31	106	10998	0.930	1235	26	0.063	2.1%	Pb loss, used lowest 204		
SE18B272	1485	28	1331	29	1341	30	1485	28	0.231	2.2%	0.093	3.0%	2.961	4.32	0.10	0.00	13	1	4	60	64	26	0	8144	0.938	1359	31	0.070	2.3%	Pb loss		
AU21E135	1592	15	1592	15	1595	15	1620	18	0.281	1.0%	0.100	1.0%	3.860	3.56	0.03	0.00	71	7	13	152	244	4	98	11038	0.962	1589	24	0.082	1.5%	ok		
AU21E112	1631	13	1474	12	1487	13	1631	13	0.259	0.9%	0.100	0.7%	3.591	3.86	0.03	0.00	82	8	21	275	321	11	235	12107	0.952	1510	19	0.078	1.3%	Minor Pb loss		
AU21E136	1635	19	1036	12	1067	13	1635	19	0.180	1.2%	0.101	1.0%	2.498	5.55	0.07	0.01	118	12	22	469	667	66	995	11031	0.914	949	17	0.048	1.8%	Pb loss, used lowest 204		
SE18B278	1651	11	1446	15	1462	16	1651	11	0.255	1.1%	0.101	1.2%	3.563	3.93	0.04	0.02	56	6	23	297	218	13	70	10754	0.949	1458	20	0.075	1.3%	Pb loss		
SE18B276	1657	18	1185	33	1214	35	1657	18	0.207	2.9%	0.102	1.9%	2.910	4.82	0.14	0.00	17	2	4	70	91	25	46	9885	0.927	1269	28	0.065	2.2%	Pb loss		
SE18B271	1663	6	872	8	907	9	1663	6	0.151	1.0%	0.102	0.7%	2.127	6.62	0.06	0.12	382	39	24	1099	2677	549	3766	12774	0.901	470	7	0.024	1.4%	Pb loss, minor ²⁰⁴ Pb		
AU21E122	1671	27	1101	25	1134	26	1671	27	0.192	2.3%	0.103	1.5%	2.720	5.20	0.12	0.01	30	3	13	216	172	39	215	9528	0.920	1260	21	0.064	1.7%	Pb loss, used lowest 204		
AU21E109	1677	15	1178	14	1209	15	1677	15	0.206	1.2%	0.103	0.8%	2.927	4.85	0.06	0.02	194	20	20	538	1041	97	866	12047	0.927	826	13	0.042	1.5%	Pb loss, off concordia, used lowest 204		
AU21E113	1703	17	1111	19	1146	20	1703	17	0.195	1.7%	0.104	0.9%	2.799	5.14	0.09	0.00	92	10	18	382	458	31	880	12058	0.921	871	16	0.044	1.8%	Pb loss, used least discordant interval		
AU21E131	1706	22	1397	22	1421	23	1706	22	0.247	1.6%	0.105	1.2%	3.554	4.05	0.07	0.00	112	12	14	241	521	35	247	12083	0.946	1264	25	0.065	1.9%	Pb loss, used lowest 204, small interval		
AU21E108	1708	21	1708	21	1708	21	1698	22	0.303	1.2%	0.104	1.2%	4.354	3.30	0.04	0.01	31	3	5	62	110	32	10	10217	0.973	1674	27	0.086	1.6%	brought to concordia		
AU21E140	1713	20	1619	17	1628	18	1713	20	0.287	1.1%	0.105	1.1%	4.155	3.48	0.04	0.01	66	7	8	107	251	5	49	7140	0.965	1644	28	0.085	1.7%	slight Pb loss		
SE18B269	1733	7	1648	14	1656	15	1733	7	0.293	0.9%	0.106	0.8%	4.284	3.41	0.03	0.00	90	10	7	89	320	5	24	12520	0.968	1581	24	0.081	1.5%	slight Pb loss		
AU21E121	1750	19	1750	19	1751	19	1765	27	0.312	1.1%	0.108	1.5%	4.646	3.20	0.04	0.01	39	4	7	81	134	3	33	10010	0.977	1782	29	0.092	1.6%	Took concordant section		
SE18B273	1750	12	1069	13	1108	14	1750	12	0.187	1.3%	0.107	1.3%	2.767	5.33	0.07	0.06	145	16	18	372	761	131	819	11700	0.918	911	19	0.046	2.0%	Pb loss, chose lowest ²⁰⁴ Pb		
SE18B277	1781	12	1660	20	1672	21	1781	12	0.296	1.2%	0.109	1.3%	4.447	3.38	0.04	0.00	53	6	11	125	178	13	152	9866	0.969	1645	24	0.085	1.5%	Pb loss		
AU21E129	1782	15	1513	15	1536	15	1782	15	0.269	1.0%	0.109	0.8%	4.044	3.72	0.04	0.01	109	12	8	141	434	8	303	11656	0.956	1177	19	0.060	1.6%	Pb loss		
AU21E128	1790	16	1790	16	1790	16	1793	10	0.320	0.9%	0.110	0.6%	4.838	3.12	0.03	0.00	118	13	7	82	376	9	19	12387	0.981	1795	27	0.093	1.5%	ok		
SE18B279	1791	17	1791	17	1791	17	1788	9	0.320	1.0%	0.109	0.9%	4.828	3.12	0.03	0.02	51	6	8	83	164	6	7	10840	0.981	1790	26	0.093	1.4%	ok		
SE18B274	1796	15	1722	22	1730	22	1796	15	0.308	1.3%	0.110	1.7%	4.661	3.25	0.04	0.02	25	3	5	56	80	21	82	10698	0.975	1758	31	0.091	1.8%	very slight Pb loss		
SE18B283	1798	15	1798	15	1799	15	1801	7	0.322	0.9%	0.110	0.8%	4.884	3.11	0.03	0.01	67	7	4	47	216	10	4	12420	0.982	1805	27	0.093	1.5%	ok		
SE18B281	1801	17	1783	30	1785	31	1801	17	0.319	1.7%	0.110	1.8%	4.841	3.14	0.05	0.02	25	3	5	57	79	57	1750	10405	0.980	1862	38	0.097	2.0%	Slight Pb loss, Fe-Ti phase present		
SE18B280	1803	7	1552	13	1575	14	1803	7	0.277	0.9%	0.110	0.7%	4.206	3.61	0.03	0.00	88	10	22	286	334	34	2976	10882	0.960	1553	20	0.080	1.3%	Pb loss, Fe rich phase throughout		
AU21E120	1811	21	1163	14	1205	15	1811	21	0.206	1.2%	0.111	1.1%	3.137	4.87	0.06	0.06	200	22	13	308	929	79	889	13669	0.926	789	15	0.040	1.9%	Pb loss, used lowest 204		
SE18B275	1825	17	1217	17	1259	17	1825	17	0.216	1.4%	0.112	1.9%	3.317	4.64	0.06	0.01	40	4	10	126	196	14	37	8998	0.931	1618	27	0.083	1.7%	Pb loss		
SE18B285	1828	12	907	14	952	16	1828	12	0.159	1.6%	0.112	1.4%	2.452	6.28	0.10	0.07	46	5	11	243	297	16	13023	9311	0.905	897	16	0.045	1.8%	Pb loss, minor ²⁰⁴ Pb		
AU21E116	1870	19	1849	20	1851	20	1870	19	0.333	1.1%	0.114	1.1%	5.245	3.01	0.03	0.00	60	7	13	133	174	20	7	10221	0.987	1801	27	0.093	1.5%	Pb loss @ begin		
AU21E118	1876	16	1609	16	1635	17	1876	16	0.289	1.0%	0.115	0.9%	4.567	3.46	0.04	0.00	55	6	24	289	189	13	98	12331	0.966	1541	21	0.079	1.4%	Th zoning, Pb loss		
AU21E126	1922	20	1880	22	1885	22	1922	20	0.340	1.2%	0.118	1.1%	5.512	2.94	0.03	0.00	64	7	9	82	179	13	47	10789	0.990	2033	33	0.106	1.6%	Very slight Pb loss		

Table 4. Isotopic and age data from LA-ICPMS analysis of zircons in samples R018223 from the Luina Group south of Luina.

Analysis	Preferred age		±1 ster		206Pb/238U age (207 corr)		±1 ster		206Pb/238U		±1 ster		207Pb/206Pb age		±1 ster		206Pb/238U ratio		±1 RSE		207Pb/206Pb ratio		±1 RSE		207Pb/235U ratio (calc)		238U/206Pb ratio		±1 std err		204Pb (ppm)		206Pb (ppm)		207Pb (ppm)		208Pb (ppm)		232Th (ppm)		238U (ppm)		49Ti (ppm)		56Fe (ppm)		176Hf (ppm)		common Pb at age of zirc		208Pb/232Th age		±1 ster		208Pb/232Th ratio		±1 RSE		Notes
	Age	σ	Age	σ	Age	σ	Age	σ	Age	σ	Age	σ	Age	σ	Age	σ	Age	σ	Age	σ	Age	σ	Age	σ	Age	σ	Age	σ	Age	σ	Age	σ	Age	σ	Age	σ	Age	σ	Age	σ	Age	σ	Age	σ	Age	σ	Age	σ	Age	σ	Age	σ							
R018223 (2013-388) Crescent Spur Sst																																																											
SE18B325	358	5	358	5	369	5	1106	16	0.059	1.4%	0.076	1.6%	0.620	16.99	0.23	0.12	61	5	13	971	1096	32	1439	11895	0.860	287	6	0.014	2.0%	common Pb																													
AU21E184	450	6	450	6	451	6	572	37	0.073	1.3%	0.059	1.7%	0.591	13.79	0.18	0.01	34	2	3	108	484	3	316	12141	0.866	548	11	0.016	2.9%	took most concordant interval																													
MY04C326	482	7	482	7	484	8	633	22	0.078	1.6%	0.061	1.0%	0.654	12.81	0.20	0.01	98	6	6	689	1442	25	692	12412	0.869	183	4	0.023	2.4%	Pb loss in 2nd half																													
AU21E179	521	9	521	9	525	10	762	35	0.085	1.8%	0.065	1.6%	0.756	11.79	0.22	0.00	58	4	2	322	666	14	423	14371	0.872	123	4	0.024	2.3%	Off concordia, common Pb																													
SE18B322	536	8	536	8	536	8	565	30	0.087	1.4%	0.059	2.8%	0.705	11.53	0.17	0.00	23	1	5	180	265	7	892	10987	0.872	523	12	0.008	2.8%	ok																													
MY04C277	544	5	544	5	544	5	555	27	0.088	0.9%	0.059	1.3%	0.713	11.35	0.10	0.00	21	1	3	120	236	11	23	10414	0.873	546	9	0.047	2.7%	ok																													
MY04C293	556	5	556	5	557	5	628	33	0.090	1.0%	0.061	1.6%	0.755	11.08	0.11	0.01	23	1	2	74	246	4	9	13003	0.874	521	12	0.052	2.3%	Pb/U age																													
MY04C306	557	4	557	4	558	4	609	32	0.090	0.8%	0.060	1.5%	0.750	11.06	0.09	0.02	40	2	7	239	420	8	531	10445	0.874	535	9	0.037	3.5%	ok																													
MY04C278	559	29	347	10	349	10	559	29	0.056	2.8%	0.059	1.3%	0.451	17.96	0.50	0.02	131	8	4	488	2208	14	2626	8853	0.859	169	5	0.025	2.9%	Pb loss, slight common Pb																													
MY04C274	561	5	561	5	562	5	584	21	0.091	0.8%	0.059	0.9%	0.747	10.98	0.09	0.00	112	7	1	175	1170	11	230	15451	0.874	83	5	0.028	2.2%	common Pb in 1st hal																													
AU21E175	570	8	570	8	576	8	870	54	0.093	1.3%	0.068	2.6%	0.876	10.71	0.14	0.03	31	2	6	229	362	15	567	12147	0.875	566	13	0.006	3.3%	Variable U/Pb																													
MY04C330	590	7	590	7	591	7	612	47	0.096	1.3%	0.060	2.2%	0.797	10.42	0.13	0.02	44	3	5	167	434	7	37	14101	0.876	568	15	0.073	6.2%	Pb loss in middle																													
MY04C303	591	7	591	7	598	8	923	43	0.097	1.3%	0.070	2.1%	0.936	10.28	0.13	0.03	39	3	9	332	383	5	103	12667	0.877	497	14	0.058	1.9%	common Pb, 204 corr brings to concordia																													
AU21E203	609	6	609	6	611	6	735	35	0.100	1.0%	0.064	1.6%	0.875	10.05	0.10	0.02	25	2	3	98	254	8	19	12618	0.878	592	11	0.024	4.4%	Variable U/Pb																													
SE18B344	621	10	621	10	626	10	868	30	0.102	1.6%	0.068	2.9%	0.956	9.80	0.15	0.01	13	1	0	5	122	5	9	11150	0.879	1425	88	0.020	2.3%	off concordia, likely due to common Pb																													
MY04C323	644	4	644	4	644	4	660	21	0.105	0.7%	0.062	1.0%	0.892	9.52	0.06	0.00	22	1	5	151	211	15	0	12816	0.880	637	9	0.060	1.5%	ok																													
SE18B345	658	7	658	7	658	7	635	17	0.107	1.0%	0.061	1.6%	0.902	9.31	0.10	0.00	33	2	4	124	316	15	9	12483	0.882	639	12	0.035	2.8%	ok																													
AU21E197	718	7	718	7	718	8	718	28	0.118	1.0%	0.063	1.3%	1.029	8.48	0.09	0.01	37	2	2	54	319	2	20	13408	0.886	699	14	0.032	2.0%	ok																													
SE18B326	839	11	839	11	843	12	959	22	0.140	1.4%	0.071	2.1%	1.368	7.16	0.10	0.00	36	3	6	135	256	46	561	11000	0.896	849	20	0.009	2.0%	mix along concordia @ beginning																													
SE18B321	852	10	852	10	854	11	916	20	0.142	1.3%	0.070	1.9%	1.358	7.06	0.09	0.01	26	2	2	54	198	7	17	10971	0.897	862	23	0.028	2.1%	slightly off concordia -common Pb?																													
MY04C273	898	19	654	6	659	7	898	19	0.108	1.0%	0.069	0.9%	1.024	9.29	0.09	0.01	61	4	4	161	584	7	301	13743	0.882	480	21	0.016	2.3%	Pb loss, some common Pb																													
AU21E177	967	12	967	12	970	13	1041	42	0.162	1.3%	0.074	2.1%	1.656	6.16	0.08	0.02	31	2	3	61	214	2	51	13236	0.906	962	26	0.040	1.9%	slight common Pb																													
MY04C279	977	39	619	10	627	11	977	39	0.102	1.7%	0.072	1.9%	1.009	9.79	0.17	0.01	15	1	1	33	145	6	4	12634	0.879	731	25	0.056	2.4%	Pb loss, slight common Pb																													
MY04C310	979	7	979	7	981	7	1034	18	0.164	0.7%	0.074	0.9%	1.671	6.08	0.04	0.00	38	3	7	161	229	8	13	10283	0.907	826	12	0.030	1.8%	ok																													
AU21E178	982	9	982	9	987	10	1093	21	0.165	1.0%	0.076	1.1%	1.732	6.05	0.06	0.02	56	4	5	109	347	1	40	11493	0.908	956	18	0.030	1.9%	Slight common Pb																													
AU21E191	992	9	992	9	993	9	1027	14	0.167	0.9%	0.073	0.7%	1.687	6.00	0.05	0.01	101	7	25	513	621	17	29	10851	0.908	965	13	0.044	2.5%	ok																													
AU21E200	1015	11	1015	11	1015	11	1000	33	0.171	1.1%	0.073	1.6%	1.706	5.86	0.06	0.00	17	1	3	68	100	8	5	8393	0.910	1006	16	0.134	1.5%	ok																													
SE18B340	1015	11	1015	11	1019	11	1106	17	0.171	1.1%	0.076	1.7%	1.805	5.84	0.07	0.03	28	2	6	128	171	18	332	9595	0.910	988	16	0.092	1.3%	common Pb, use U/Pb age																													
AU21E202	1031	13	1031	13	1032	13	1051	35	0.174	1.3%	0.074	1.8%	1.779	5.76	0.07	0.00	38	3	6	116	210	4	5	9484	0.911	1012	18	0.060	1.8%	ok																													
AU21E194	1031	12	1031	12	1033	13	1081	37	0.174	1.2%	0.075	1.8%	1.809	5.75	0.07	0.00	38	3	6	133	238	12	77	11724	0.911	1041	17	0.043	2.4%	Pb loss in 2nd half																													
MY04C320	1037	7	1037	7	1038	7	1069	13	0.175	0.7%	0.075	0.6%	1.808	5.72	0.04	0.01	138	10	16	339	773	8	168	10796	0.912	903	12	0.078	2.2%																														
SE18B342	1044	39	774	14	782	14	1044	39	0.129	1.8%	0.074	3.9%	1.317	7.76	0.14	0.00	4	0	1	24	34	22	133	7814	0.891	689	20	0.026	2.2%																														
MY04C297	1050	10	1050	10	1063	10	1326	17	0.179	0.9%	0.085	0.9%	2.113	5.58	0.05	0.06	113	10	27	702	663	14	710	10921	0.914	792	15	0.045	1.4%																														
MY04C319	1051	8	1051	8	1051	8	1054	17	0.177	0.8%	0.074	0.8%	1.819	5.65	0.05	0.00	106	8	19	361	573	8	164	10996	0.913	1015	14	0.048	1.8%																														
MY04C314	1052	8	1052	8	1054	8	1091	18	0.178	0.7%	0.076	0.9%	1.858	5.63	0.04	0.00	57	4	6	110	338	56	3170	10910	0.913	1078	18	0.048	1.6%																														
MY04C302	1057	7	1057	7	1058	8	1075	13	0.178	0.7%	0.075	0.6%	1.850	5.61	0.04	0.00	51	4	10	183	291	6	20	9212	0.914	1065	14	0.053	1.3%																														
MY04C325	1058	6	1058	6	1058	6	1047	12	0.178	0.6%	0.074	0.6%	1.825	5.61	0.03	0.00	73	5	8	152	421	9	38	11721	0.914	1032	13	0.122	2.0%																														
MY04C285	1060	23	1031	12	1033	13	1060	23	0.174	1.2%	0.075	1.1%	1.789	5.76	0.07	0.01	53	4	2	47	344	10	34	13182	0.911	1035	27	0.027	1.7%																														
MY04C329	1062	7	1062	7	1062	7	1037	13	0.179	0.7%	0.074	0.6%	1.823	5.58	0.04	0.01	88	7	21	409	522	6	149	8237	0.914	1046	14	0.050	1.7%																														
MY04C316	1065	6	1065	6	1065	7	1047	11	0.180	0.6%	0.074	0.6%	1.839	5.56	0.03	0.00	106	8	10	192	619	5	29	12654	0.914	1064	14	0.079	1.4%																														
MY04C305	1066	8	1066	8	1066	8	1023	17	0.180	0.8%	0.073	0.8%	1.818	5.56	0.04	0.00	32	2	5	87	183	12	9	11969	0.914	1092	16	0.051	1.6%																														
MY04C298	1077	16	852	10	859	11	1077	16	0.143	1.2%	0.075	0.8%	1.481	7.01	0.09	0.03	140	10	6	400	991	20	443	14601	0.897	320	7	0.053	1.7%																														
SE18B330	1081	12	1081	12	1082	13	1113	20	0.183	1.2%	0.077	2.0%	1.933	5.47	0.06	0.00	22	2	3	65	127	5	3	10680	0.916	1095	22	0.049	2.7%																														
MY04C301	1081	26	785	8	794	8																																																					

Table 4. (cont.)

Analysis	Preferred age	Pb/U ratios and RSE														Pb/Pb ratios and RSE										Notes			
		±1 ster	²⁰⁶ Pb/ ²³⁸ U age (207 corr)	±1 ster	²⁰⁶ Pb/ ²³⁸ U	±1 ster	²⁰⁷ Pb/ ²⁰⁶ Pb age	±1 ster	²⁰⁶ Pb/ ²³⁸ U ratio	±1 RSE	²⁰⁷ Pb/ ²⁰⁶ Pb ratio	±1 RSE	²⁰⁷ Pb/ ²³⁵ U ratio (calc)	²³⁸ U/ ²⁰⁶ Pb ratio	±1 std err	²⁰⁴ Pb (ppm)	²⁰⁶ Pb (ppm)	²⁰⁷ Pb (ppm)	²⁰⁸ Pb (ppm)	²³² Th (ppm)	²³⁸ U (ppm)	⁴⁹ Ti (ppm)	56Fe (ppm)	¹⁷⁸ Hf (ppm)	common Pb at age of zirc		²⁰⁸ Pb/ ²³² Th age	±1 ster	²⁰⁸ Pb/ ²³² Th ratio
SE18B339	1084	11	1084	11	1084	11	1082	13	0.183	1.0%	0.075	1.3%	1.905	5.46	0.06	0.00	43	3	7	127	239	11	15	11531	0.916	1054	15	0.059	2.8%
AU21E193	1086	10	1086	10	1086	10	1097	21	0.183	0.9%	0.076	1.0%	1.925	5.45	0.05	0.01	33	2	7	128	185	6	22	11740	0.916	1098	15	0.042	1.4%
MY04C281	1093	7	1093	7	1094	7	1101	13	0.185	0.6%	0.076	0.6%	1.943	5.41	0.04	0.00	58	4	11	205	321	15	488	9524	0.917	1086	14	0.026	2.3%
MY04C291	1096	11	1096	11	1098	11	1139	35	0.186	1.0%	0.078	1.7%	1.990	5.38	0.05	0.00	39	3	11	186	199	10	87	10673	0.917	1073	19	0.053	1.8%
MY04C292	1097	7	1097	7	1098	7	1125	14	0.186	0.6%	0.077	0.7%	1.975	5.39	0.03	0.00	49	4	4	76	269	9	290	7485	0.917	1129	16	0.053	1.6%
AU21E183	1101	16	1065	9	1067	10	1101	16	0.180	0.9%	0.076	0.8%	1.892	5.56	0.05	0.00	64	5	16	290	355	8	46	11215	0.914	1055	14	0.053	1.6%
MY04C315	1104	15	1156	8	1156	8	1104	15	0.196	0.7%	0.076	0.8%	2.066	5.09	0.04	0.00	47	4	8	149	251	17	3	12380	0.922	1104	15	0.004	6.4%
MY04C327	1105	8	1105	8	1105	8	1095	18	0.187	0.7%	0.076	0.9%	1.959	5.35	0.04	0.00	23	2	5	90	120	15	60	10194	0.918	1061	19	0.055	1.8%
AU21E180	1106	15	1106	15	1108	16	1144	40	0.187	1.4%	0.078	2.0%	2.013	5.33	0.07	0.02	44	3	5	80	224	23	769	11152	0.918	1166	26	0.028	2.6%
SE18B328	1106	17	1106	17	1109	17	1171	26	0.188	1.5%	0.079	2.7%	2.044	5.33	0.08	0.00	14	1	2	37	73	11	3	9390	0.918	1157	32	0.055	1.6%
SE18B329	1108	11	1108	11	1110	11	1154	12	0.188	1.0%	0.078	1.2%	2.029	5.32	0.05	0.03	99	8	12	253	579	5	22	11732	0.918	1048	17	0.049	1.3%
MY04C321	1110	16	983	8	988	9	1110	16	0.166	0.9%	0.077	0.8%	1.749	6.04	0.05	0.01	74	6	13	309	487	15	381	12009	0.908	884	13	0.059	2.2%
SE18B332	1132	11	1132	11	1132	11	1114	9	0.192	1.0%	0.077	0.9%	2.031	5.21	0.05	0.00	76	6	2	57	417	10	53	12674	0.920	840	20	0.054	1.3%
MY04C296	1142	29	1057	10	1061	11	1142	29	0.179	1.0%	0.078	1.5%	1.919	5.59	0.06	0.01	23	2	5	103	138	7	11	9476	0.914	1037	18	0.046	1.4%
AU21E186	1147	25	852	9	862	9	1147	25	0.143	1.0%	0.078	1.3%	1.539	6.99	0.07	0.00	43	3	8	250	298	19	1025	11507	0.897	633	13	0.056	2.0%
SE18B324	1147	33	494	8	506	8	1147	33	0.082	1.6%	0.078	3.3%	0.879	12.24	0.19	0.04	63	5	16	671	760	56	2739	10666	0.870	452	11	0.053	2.7%
MY04C324	1148	20	1059	8	1063	9	1148	20	0.179	0.8%	0.078	1.0%	1.930	5.58	0.05	0.01	56	4	7	151	346	5	67	12469	0.914	1007	17	0.032	1.4%
MY04C322	1157	8	1157	8	1157	8	1129	15	0.197	0.7%	0.077	0.7%	2.095	5.09	0.04	0.01	41	3	5	100	216	5	31	11008	0.922	978	22	0.057	1.4%
AU21E188	1160	21	1048	10	1053	10	1160	21	0.177	0.9%	0.079	1.1%	1.921	5.64	0.05	0.01	47	4	14	267	271	7	21	10301	0.913	1043	14	0.071	1.7%
SE18B334	1165	9	935	8	944	8	1165	9	0.158	0.9%	0.079	0.9%	1.712	6.34	0.06	0.02	83	7	10	324	527	28	190	10840	0.904	597	11	0.089	1.2%
AU21E182	1170	19	1111	12	1113	12	1170	19	0.189	1.1%	0.079	1.0%	2.052	5.30	0.06	0.00	107	8	11	232	618	6	114	13649	0.918	1043	18	0.027	1.7%
AU21E185	1184	13	1184	13	1184	14	1201	30	0.202	1.1%	0.080	1.5%	2.229	4.96	0.06	0.00	66	5	3	58	366	4	22	13570	0.924	1144	27	0.051	1.8%
AU21E199	1208	11	1208	11	1209	12	1224	32	0.206	1.0%	0.081	1.6%	2.307	4.85	0.05	0.00	123	10	19	283	573	3	119	13165	0.926	1190	20	0.054	1.3%
AU21E198	1228	58	974	17	984	18	1228	58	0.165	1.8%	0.081	3.0%	1.848	6.06	0.11	0.02	14	1	3	46	80	3	2	8799	0.907	1105	27	0.058	2.4%
MY04C287	1247	31	689	8	705	9	1247	31	0.116	1.2%	0.082	1.6%	1.307	8.66	0.11	0.00	61	5	15	616	500	15	599	12208	0.885	476	11	0.061	1.7%
AU21E187	1283	17	1154	10	1161	11	1283	17	0.197	0.9%	0.084	0.9%	2.274	5.07	0.05	0.01	82	7	8	180	424	5	189	12533	0.922	953	15	0.055	1.7%
AU21E195	1388	15	1388	15	1390	16	1424	28	0.241	1.1%	0.090	1.5%	2.984	4.16	0.05	0.00	26	2	5	70	104	14	101	10651	0.943	1383	23	0.056	1.4%
AU21E181	1416	19	1416	19	1416	20	1396	24	0.246	1.4%	0.089	1.3%	3.002	4.07	0.06	0.00	36	3	6	73	142	23	228	12240	0.945	1442	27	0.084	2.4%
AU21E196	1429	52	552	9	573	9	1429	52	0.093	1.7%	0.090	2.7%	1.156	10.75	0.18	0.06	48	4	8	506	544	28	1359	12267	0.875	325	9	0.055	1.3%
AU21E192	1456	48	905	16	928	16	1456	48	0.155	1.8%	0.091	2.5%	1.951	6.46	0.11	0.01	8	1	2	39	52	57	6947	9626	0.903	1032	24	0.052	1.4%
MY04C304	1488	35	1058	13	1080	14	1488	35	0.182	1.3%	0.093	1.8%	2.339	5.48	0.07	0.00	21	2	5	99	123	17	152	8457	0.915	1146	22	0.035	2.0%
MY04C282	1543	16	1119	11	1142	12	1543	16	0.194	1.1%	0.096	0.9%	2.559	5.16	0.05	0.00	68	7	15	264	382	6	54	10702	0.921	1173	18	0.054	1.4%
AU21E176	1682	28	1038	19	1072	20	1682	28	0.181	1.9%	0.103	1.5%	2.574	5.53	0.10	0.01	73	7	9	201	425	27	478	11793	0.915	933	25	0.054	1.7%
SE18B323	1710	20	1710	20	1712	20	1730	10	0.304	1.2%	0.106	1.1%	4.443	3.29	0.04	0.02	150	16	15	266	484	11	525	10153	0.973	1087	19	0.052	1.3%
MY04C272	1717	16	1578	12	1590	12	1717	16	0.280	0.8%	0.105	0.9%	4.057	3.57	0.03	0.00	48	5	10	136	178	17	154	11131	0.961	1532	21	0.074	1.8%
MY04C328	1764	12	1725	13	1729	13	1764	12	0.308	0.8%	0.108	0.6%	4.576	3.25	0.03	0.01	148	16	41	447	459	11	8	9699	0.975	1714	21	0.051	1.6%
AU21E201	1777	20	1777	20	1779	20	1795	26	0.318	1.1%	0.110	1.4%	4.807	3.15	0.03	0.00	49	5	3	38	168	10	3	12902	0.980	1640	39	0.042	2.4%
MY04C283	1794	14	1553	13	1575	13	1794	14	0.277	0.9%	0.110	0.8%	4.186	3.61	0.03	0.00	194	21	25	393	666	74	764	12213	0.960	1180	21	0.122	1.4%
SE18B343	1833	20	1602	39	1624	40	1833	20	0.286	2.5%	0.112	2.2%	4.424	3.49	0.09	0.00	26	3	8	117	105	18	19	8791	0.965	1524	34	0.054	1.3%
SE18B333	1894	9	1549	14	1581	15	1894	9	0.278	1.0%	0.116	0.7%	4.443	3.60	0.03	0.03	214	25	8	169	756	13	147	18009	0.961	880	22	0.134	1.2%
MY04C295	2145	10	1800	13	1843	14	2145	10	0.331	0.8%	0.134	0.6%	6.095	3.02	0.02	0.00	47	6	9	102	145	18	211	12240	0.986	1786	23	0.053	1.3%
MY04C284	2309	12	2348	18	2348	17	2309	12	0.439	0.7%	0.147	0.7%	8.895	2.28	0.02	0.00	48	7	10	87	115	8	18	11987	1.039	2328	32	0.050	2.2%
MY04C300	2511	5	2559	18	2559	17	2511	5	0.487	0.7%	0.165	0.3%	11.110	2.05	0.01	0.00	213	35	22	162	445	2	56	12210	1.062	2550	32	0.032	1.8%
SE18B341	2976	8	2391	28	2544	28	2976	8	0.484	1.1%	0.219	0.6%	14.631	2.07	0.02	0.01	105	23	25	188	217	102	3504	10286	1.060	2549	38	0.056	1.5%
MY04C309	3208	6	2772	34	2930	31	3208	6	0.575	1.1%	0.254	0.4%	20.122	1.74	0.02	0.01	135	34	12	109	256	8	214	10923	1.102	2334	47	0.056	1.3%

